Point-by-point response to reviewer comment on manuscript acp-2020-443 “Impact of organic acids on chloride depletion of inland transported sea spray aerosols”

We appreciate the two anonymous reviewers for their constructive comments to improve the manuscript. We have addressed every comment and made changes to improve the manuscript.
With kindest regards,
By Bojiang Su on behalf of all authors

Note
Referee Comments in black.
Authors’ Response in blue.
Changes in manuscript in Red.

Anonymous Referee #1

General comments

This paper discusses the depletion of chloride in sea spray aerosol (SSA) particles based on a field observation of atmospheric aerosol during the East Asian summer monsoon using a single particle aerosol mass spectrometer. The authors claim that up to 34% of chloride depression could be explained by organic acids. They also claim that SSA of biogenic origin exhibits chloride depression that is distinctly different from that of commonly observed aged SSA, and infer that organic coatings on SSA could influence on the heterogeneous reactivity of SSA particles. The subject of this study is important to understand the chemical processes of SSA and also their role in the atmosphere.

Although the findings from this study are potentially significant, the conclusions are not fully supported by the experimental evidence provided in the current version of the manuscript. For example, in the quantitative analysis of the contributions of inorganic and organic acids on chloride depression, no explanation is provided about possible different sensitivity of the mass spectral analysis to different compounds. Further, the comparison of Cl/Na from mass spectra and that from mass concentrations was performed by omitting a substantial fraction of data points, without an adequate explanation on the rationale of the omission. To draw a solid conclusion from the data set presented in this paper, a thorough revision is necessary. More specific comments are listed below.

Author’s Response: We appreciate the valuable time and efforts from the referee to improve the manuscript. Please see below for the point-by-point response to reviewers’ comments.

R1-C1: For example, in the quantitative analysis of the contributions of inorganic and organic acids on chloride depression, no explanation is provided about possible different sensitivity of the mass spectral analysis to different compounds.

Author's Response: Thanks for the referee's comment. In the revised manuscript, we have added a new section to discuss the quantitative analysis of single particle aerosol mass spectrometer. In addition, the possible different sensitivity of different species (especially Na, Cl, nitrate, sulfate and organics) in single particle mass spectrometry was also discussed.

"Using single particle mass spectrometry (SPMS) alone is subjected to the transmission efficiencies of particles through the aerodynamic lens, the possible selectivity and matrix effects on chemical components, resulting in inaccuracies of the number concentration, size distribution and chemical composition of the ambient aerosols (Gross et al., 2000; Qin et al., 2006; Pratt and Prather, 2012). Thus, a comparison analysis based on the obtained particle counts, size distributions and peak area / relative peak area via SPMAS in this study should be considered as the semi-quantitative analysis from statistical perspective (Hinz et al., 2005; Jeong et al., 2011; Healy et al., 2012; Zhou et al., 2016). More detailed discussion for the semi-quantitative analysis of SSA particles could be seen in *Supplement*."

"1. Semi-quantitative analysis of SSA particles (in *supplement*)

"Using single particle mass spectrometry (SPMS) alone is subjected to the transmission efficiencies of particles through the aerodynamic lens, the possible selectivity and matrix effects on chemical components, resulting in inaccuracies of the number concentration, size distribution and chemical composition of the ambient aerosols (Gross et al., 2000; Qin et al., 2006; Pratt and Prather, 2012).

Despite this, some species (e.g., sulfate, nitrate, sodium, ammonium, elemental carbon and organic carbon) presented relative strong correlations between peak area / relative peak area (data set from SPMS) and mass concentration (data set from other measurements such as micro-orifice uniform deposit impactor (MOUDI)), which indicated the real ambient condition could be reflected by SMPS in some extent (Qin et al., 2006; Jeong et al., 2011; Healy et al., 2012; Healy et al, 2013; Zhou et al., 2016). Besides, similar results of correlation analysis on Na^+, Cl^-, K^+ for SSA particles (< 2 μm) were also obtained, which suggested no significant additional composition effect for the desorption and ionization process (Dall'Osto et al., 2006).

In addition, for the core-shell structure of the most SSA particles (Collins et al., 2014; Chi et al., 2015), the pulse energy of the desorption and ionization laser via SPMS was influential for the selectivity of the detected components on the surface of the particles (Woods et al., 2002; Cai et al., 2006; Zelenyuk et al., 2008). Sultana et al. (2017) suggested that higher laser energy (> 1 mJ) could result in greater sodium signal, indicating more complete particle desorption and ionization. And lower laser energy (< 1 mJ) could be more likely to generate greater contribution to ion signature from the coating components such as organic species (Sultana et al., 2017). In order to reduce the impact of laser power on organic species, relative low laser energy (0.5 ± 0.05 mJ) was applied in this study.

Thus, a comparison analysis based on the obtained particle counts, size distributions and peak area / relative peak area via SPMAS in this study should be considered as the semi-quantitative analysis from statistical perspective (Hinz et al., 2005; Healy et al., 2012; Zhou et al., 2016)."

R1-C2: Further, the comparison of Cl/Na from mass spectra and that from mass concentrations was performed by omitting a substantial fraction of data points, without an adequate explanation on the rationale of the omission.

Author's Response: Thanks for the referee's comment. We have reviewed the original data set from the mass concentration and the mass spectral analysis. Only 3 data points should be excluded due to the maximum, minimum and the abnormal value. This part was reconsidered and rewritten in the revised manuscript as shown below:

"It is noted that excess $[Cl]^-$ produced by fuel combustion (Lightowlers et al., 1988) could lower the $\%Cl^-$ and high sensitivity of SPAMS to Na^+ (Gross et al., 2000) could increase the Cl / Na value. These potential inaccuracies might be more likely to explain the weak difference for the two assessment methods of ageing degree of SSA particles, which are evaluated by hourly mean peak area of Cl / Na and quantification of chloride depletion on mass concentration. Generally, the quantitative analysis of mass concentration could directly evaluate the degree of chloride depletion in SSA particles (Braun et al., 2017). We note that there are some consistencies between the two assessment methods, which are supported by a positive correlation ($r^2 = 0.22$, $p < 0.001$) (Fig. S7). Hence, the hourly mean peak area of Cl / Na could also semi – quantitatively reflect the degree of chloride depletion, in some extent."

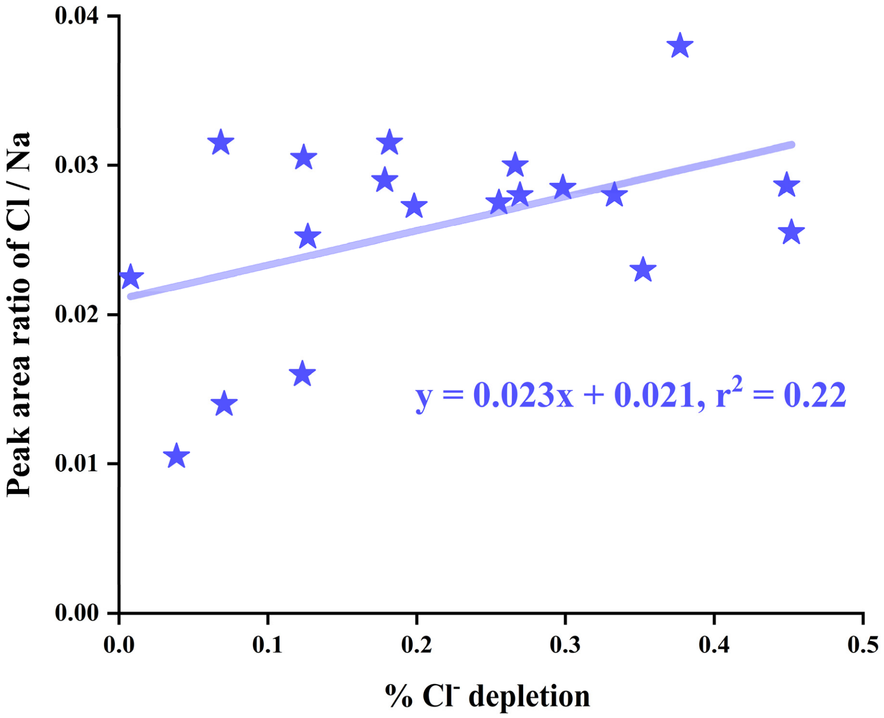

On the other hand, Fig. S7 and Table S1 were modified and their description were also rewritten as shown below:

"Fig S7. Correlation analysis of the both assessment methods of chloride depletion. These data were conducted significance test and $p < 0.001$. The correlation analysis was carried out on 19 among 22 set of data due to the rest of the maximum, minimum and the abnormal value (detailed in Table S1)."

Sampling set names	Sampling dates	Duration (min)	Na^+	Ca^{2+}	Cl^-	NO_3^-	SO_4^{2-}	Cl^-% depletion	Peak area ratio of Cl / Na
Cloud Water 1	May 11	480	0.24	0.01	0.16	1.26	1.81	0.64	0.005*
Cloud Water 2	May 26	150	1.31	0.74	0.58	5.59	9.32	0.65	0.023
Cloud Water 3	May 26	140	1.73	0.98	0.56	3.90	6.48	0.74	0.028
Cloud Water 4	May 26	180	5.24	1.80	0.99	6.41	9.65	0.87	0.025
Cloud Water 5	May 27	214	1.98	1.21	1.08	9.33	13.84	0.55	0.029
Cloud Water 6	May 30	270	1.85	1.35	0.53	8.57	13.08	0.73	0.030
Cloud Water 7	May 30	305	1.88	1.07	0.79	11.14	16.95	0.67	0.028
Cloud Water 8	May 30	515	1.68	1.22	0.83	11.59	19.32	0.55	0.026
Cloud Water 9	Jun 1	225	1.07	0.79	0.31	5.57	5.71	0.73	0.028
Cloud Water 10	Jun 2	230	0.99	0.42	0.05	2.10	3.84	0.96	0.011
Cloud Water 11	Jun 2	141	1.63	0.59	0.30	3.84	5.64	0.88	0.016
Cloud Water 12	Jun 2	134	1.44	0.46	0.15	1.85	2.63	0.93	0.014
Cloud Water 13	Jun 2	203	3.79	1.03	0.35	3.85	5.80	0.94	0.046*
$PM_{2.5}$ 1	May 14-15	1440	1.12	1.04	0.38	1.05	2.60	0.62	0.038
$PM_{2.5}$ 2	May 18-19	1406	1.46	0.47	0.40	1.80	4.75	0.82	0.032
$PM_{2.5}$ 3	May 19-20	1423	0.45	0.22	0.07	2.07	5.09	0.88	0.031
$PM_{2.5}$ 4	May 20-21	1366	0.70	0.22	0.21	3.22	4.70	0.80	0.027
$PM_{2.5}$ 5	May 21-22	1431	0.48	0.18	0.13	2.11	3.52	0.82	0.029
$PM_{2.5}$ 6	May 22-23	1414	0.57	0.16	0.06	0.97	2.94	0.93	0.032
$PM_{2.5}$ 7	May 24-25	1419	0.72	0.21	0.17	2.59	4.22	0.80	0.054*
$PM_{2.5}$ 8	May 26-27	1391	0.72	0.47	0.25	2.36	3.20	0.70	0.029
$PM_{2.5}$ 9	May 29-30	1421	0.51	0.03	0.01	0.35	1.84	0.99	0.023
Mean			1.43	0.67	0.38	4.16	6.68	0.78	0.026

* These data are excluded because of the maximum (0.054), minimum (0.005) and abnomal value (0.046).

"Table S1. The major ions, chloride depletion (%Cl^-) and hourly mean peak area ratio of Cl / Na in the sample of cloud water and $PM_{2.5}$ during sampling period. The mass concentrations (μg m^{-3}) of Na^+, Ca^{2+}, Cl^-, NO_3^- and SO_4^{2-} were analyzed using an ion chromatography (Metrohm, Herisau, Switzerland). The cloud water was sampled by a Caltech Active Strand Cloud Water Collector Version 2 (CASCC2) (Modini et al., 2015), when visibility was < 3 km until the volume exceeded 250 ml. The PM2.5 was sampled using an Atmospheric particle sampler (Mingye Environmental Protection Technology Co., Ltd., China) with an inlet cyclone with a cut-off aerodynamic diameter of 2.5 μm."

In **R1-C17**, we have discussed two assessment methods of chloride depletion (i.e., Cl / Na evaluated by hourly mean peak area and quantification on mass concentration.). Generally, the quantitative analysis of mass concentration could directly evaluate the degree of chloride depletion in SSA particles. We note that there are some consistencies between the two assessment methods, which are supported by a positive correlation ($r^2 = 0.22$, $p < 0.001$). Thus, the hourly mean peak area of Cl / Na could semi–quantitatively reflect the degree of chloride depletion, in some extent.

Specific comments

R1-C3: Page 3, lines 25-26: For nitrogen and sulfur, the explanation here sounds an overstatement.

Author's Response: Thanks for pointing out this. The sentence was rewritten as "Heterogeneous reactions on sea spray aerosols (SSA) are the potential pathway to drive the circulation of chlorine, nitrogen, and sulfur in the atmosphere."

R1-C4: Page 6, line 80: Is there any experimental/theoretical evidence to support reaction R5?

Author's Response: Exactly, Wang and Laskin, (2014) reported that internally mixed nitrate particles with organic acids could result in nitrate depletion and formation of organic salts, represented as:

$NaNO_3$ *(aq)* + R-COOH *(g or aq)* ↔ HNO_3 *(g or aq)* + R-COONa *(s or aq)*

R1-C5: Page 9, lines 146-151: If both types of particles were subjected to the analysis, it should be explained explicitly.

Author's Response: Thanks for the referee's opinion. We added a sentence:

"In the following discussion, the cloud residual particles and cloud-free particles were combined as the total of detected particles."

R1-C6: Page 10, line 163: What is the exact number of groups?
Author's Response: The detected particles were clustered into 8 groups by ART-2a. The sentence was rewritten as "A total of ~2 million detected particles were clustered into 8 groups using an Adaptive Resonance Theory neural network (ART-2a) (Song and Hopke, 1999) with a vigilance factor of 0.75, a learning rate of 0.05 and a maximum of 20 iterations."

R1-C7: Page 10, line 166: To justify the identification of SSA particles, a brief explanation on the differences between SSA particles and other types of particles should be provided.
Author's Response: We agree with the referee's opinion. And we added a sentence as below:
"In single particle mass spectral fingerprints, it is the key to distinguish SSA from other groups of particles whether to present the ion signature of 23 $[Na]^+$, 46 $[Na_2]^+$, 62 $[Na_2O]^+$, 63 $[Na_2OH]^+$, 81 $[Na_2{}^{35}Cl]^+$ and 83 $[Na_2{}^{37}Cl]^+$ simultaneously. (Ault et al., 2014; Collins et al., 2014; Lin et al., 2019)."

R1-C8: Page 13, line 222: What can crystallize? The meaning of "precipitation" is not clear.
Author's Response: Ault et al. (2014) and Sultana et al. (2017) observed the types of SSA particles associated with Na-deficient and Ca-rich mass spectral signatures. This Ca-rich population may be the coating of Na-rich particles (Sultana et al., 2017), which comes from the precipitation and crystallization by calcium sulfate, calcium sulfate hydrates, and sodium calcium sulfate salts during the dehydration of seawater and seawater droplets (Xiao et al., 2008).
The relevant sentences had been rewritten as below:
"This SSA population has been previously classified as "organic-carbon dominated (OC)" (Prather et al., 2013; Collins et al., 2014), likely resulted from the coating of Na-rich SSA particles through crystallization and precipitation of Ca-containing sulfate (e.g., calcium sulfate and sodium calcium sulfate) during the dehydration of sea water and seawater droplets (Xiao et al., 2008; Sultana et al., 2017; May et al., 2018)."

R1-C9: Page 13, lines 228-229: The definition of hourly-mean peak areas in Fig. 2 is unclear.
Author's Response: Thanks for pointing out this. We have given a definition of hourly mean peak area. This part has been rewritten as:
"The linear correlations based on hourly mean peak area between Na and chloride, sulfate, nitrate, and organic acids in the SSA-Aged and SSA-Bio particles are shown in Fig. 2. Herein, hourly mean peak area was defined as the mean peak area of a component for hourly detected particles, indicating the variations of chemical composition in individual particles."

R1-C10: Page 13, lines 232-233: This explanation is reasonable if nitrate was observed less frequently for non-SSA particles.
Author's Response: Thanks for the referee's opinion. It is true that relative low number fractions of nitrate (varying from 46% to 95%) were observed in other types of particles (i.e., Aged-EC, OC, K-rich and HM) at the same field site (Lin et al., 2017). However, for SSA particles, we emphasize the significance of heterogeneous reaction $HNO_{3\,(g\ or\ aq)} + NaCl_{(s\ or\ aq)} \rightarrow NaNO3_{(aq)} + HCl_{(g\ or\ aq)}$ plays important role on chloride depletion of SSA particles during long-range transport.

R1-C11: Page 13, lines 236-238: It is difficult for readers to follow this part without an explanation about the mechanism of the suppression. Isn't it also possible that nitric acid and other acids have different reactivity to sea salts?

Author's Response: We agree with the referee's comment. For this part, we think that the relative high concentration of precursor NO_x was one of the factors in explanation of nitric acids responsible for chloride depletion.

The sentence had been rewritten as below:

"It is possible supported by the relative high concentration of its precursor NO_x (4.67 $\mu g\ m^{-3}$) in the south China sector (Wang et al., 2016; Wu et al., 2019)."

R1-C12: Page 14, lines 245-246: The expression is misleading because the result in Fig. S4 is on number basis and may not relate to the mass concentrations of different organic salts in SSA particles.

Author's Response: We agree with the referee's comment. The relevant sentence had been rewritten as below:

"The detailed mixing state (by NFs) between SSA particles and several detected organic acids, as shown in Fig. S4, indicates that formate, oxalate, malonate, and glutarate might be the dominant organic salts. This result may be associated with the wide range of occurrence of corresponding organic acids in the atmosphere (Ghorai et al., 2014; Kawamura and Bikkina, 2016)."

R1-C13: Page 14, lines 246-258: In the absence of an appropriate explanation on possible different sensitivities of this mass spectrometry to different types of chemical components (sulfate/nitrate/organics), the discussion here is questionable.

Author's Response: Thanks for the referee's comment. We have added a detailed discussion on the possible different sensitivities and matrix effect of the mass spectrometry to different chemical component (including sulfate, nitrate, chloride, sodium and organics) in *Supplement* 1. Our obtained results were based on the semi-quantitative analysis from statistical perspective. In addition, we have referred the other citations as below:

"The similar method was also introduced to evaluate the extent of chloride depletion in previous study (Ault et al., 2014)."

R1-C14: Page 14, lines 258-261: Are the peak areas here hourly mean values?

Author's Response: It is correct. To make it clear, we have rewritten the sentence as below:

"In addition, similar variations in hourly mean peak area of sulfate, nitrate and organic acids were observed in the SSA-Aged and SSA-Bio particles throughout the sampling period (Fig. S6), indicating a close connection of the formation mechanism between inorganic and organic acids."

R1-C15: Page 15, lines 264-265: Isn't there any possibility that matrix substances in the particles affect the relative sensitivity to detect Na and Cl?

Author's Response: Exactly, there is a possibility that matrix effect might be likely to affect the relative sensitivity to detect Na^+ and Cl^-. The detailed discussion of this part was supplemented in *Supplement* 1.

R1-C16: Page 15, lines 272-275: The mass concentrations of Na+ and Cl- seem to be from ion chromatography but there is no explanation about the methodology in the main manuscript.

Author's Response: Thanks for the referee's opinion. We have supplemented the explanation of methodology related to ion chromatography in this part. As shown below:

"The mass concentration of major ions (such as Na^+ and Cl^-) was analyzed using an ion chromatography (Metrohm, Herisau, Switzerland), detailed information could be found in *supplement* Table S1. The overall $\%Cl^-$ for the total SSA particles varying from 55% to 99% with an average of 78% (Table S1), which is similar to the previous field study in the PRD region reported by Chen et al. (2016)."

R1-C17: Page 15, line 280: Two assessment methods should be explained explicitly.

Author's Response: Thanks for the suggestion. We have rephrased this part to explain clearly.

"It is noted that excess $[Cl]^-$ produced by fuel combustion (Lightowlers et al., 1988) could lower the $\%Cl^-$ and high sensitivity of SPAMS to Na^+ (Gross et al., 2000) could increase the Cl / Na value. These potential inaccuracies might be more likely to explain the weak difference for the two assessment methods of ageing degree of SSA particles, which are evaluated by hourly mean peak area of Cl / Na and quantification of chloride depletion on mass concentration. Generally, the quantitative analysis of mass concentration could directly evaluate the degree of chloride depletion in SSA particles (Braun et al., 2017). We note that there are some consistencies between the two assessment methods, which are supported by a positive correlation ($r^2 = 0.22$, $p < 0.001$) (Fig. S7). Hence, the hourly mean peak area of Cl / Na could also semi – quantitatively reflect the degree of chloride depletion, in some extent."

R1-C18: Page 15, line 281-283: The analysis of the correlation is problematic because 7 among 22 set of data were omitted from the analysis without an appropriate assessment.

Author's Response: Thanks for the referee's comment. We have reviewed the original data set from the mass concentration and the mass spectral analysis. Only 3 data points should be excluded due to the maximum, minimum and the abnormal value. Thus, the correlation analysis was carried out on 19 among 22 set of data. Detailed explanation could be found in **R1-C2.**

R1-C19: Page 33, line 623: Which part of data shows a normal distribution? Why it is obtained by the logarithmic transformation?

Author's Response: The data set related to hourly mean peak area of Na, nitrate, chloride and sulfate was logarithmically transformed to follow a normal distribution. From the statistical perspective, the correlation analysis should base on the data following the normal distribution. For the peak area of single particle mass spectrometry, there is a significant difference (1 ~ 4 orders of magnitude) between maximum and minimum because of the different degree of desorption / ionization. In order to obtain the more accurate results, we thus used logarithmical transformation to make the data follow the normal distribution as possible.

R1-C20: Page 35, lines 632-635: An explanation on the box and whisker plots should be given

Author's Response: Thanks for the referee's opinion. We supplemented this part as shown below:

"Figure 4. A box and whisker plot of hourly mean peak area of Cl / Na in SSA-Aged and SSA-Bio. Herein, the Cl / Na value is applied to evaluate the ageing degree of SSA particles. There is a significant difference of Cl / Na between the SSA-Aged and SSA-Bio (1.9% versus 5.4%, by mean value, respectively). In the box and whisker plot, the lower and upper lines of the box denote the 25 and 75 percentiles, respectively. The lower and upper edges denote the 10 and 90 percentiles, respectively."

R1-C21: Page 36, lines 637-639: Isn't it more reasonable to write Cl/Na as a function of peak areas of phosphate and organic nitrogen?

Author's Response: We agree with the referee's opinion. We have rewritten this sentence as below: "Figure 5. The hourly mean peak area ratio of Cl / Na varied as a function of logarithmical peak area of phosphate (*m/z* -63 and -79) and organic nitrogen (*m/z* -26 and -42)."

R1-C22: Page 2, lines 7-11 (supplement): The association between trajectories on the map and C1-C4 should be explained. The graph superimposed on the map should also be explained.

Author's Response: Thanks for the referee's opinion. We have rewritten and reorganized this part, as shown below:

"Figure S1. Quantitative distributions of SSA particles associated with clustered 72h back trajectories of air masses at 1800m above the ground during the sampling period (from 11 May to 3 June 2018). Four major cluster trajectories of air mass (namely C1, C2, C3, C4) were calculated by Meteoinfo (Wang, 2014) and plotted by Arcgis (Esri, Environmental Systems Research Institute, Inc.). Cluster 1 (41.64%) from Indo China Peninsula and Cluster 4 (18.46%) from south China Sea crossing through Hainan Peninsula carried the most (~ 25,000) and the least (~ 5,000) SSA particles, respectively. The both from the South China Sea Cluster 2 (28.92%) and Cluster 3 (10.98%), which brought approximately 12,500 and 7,500 SSA particles respectively, were rarely affected by anthropogenic emissions before reaching the coastline. Changes in proportions of the three types of SSA particles in different clusters were slight."

R1-C23: Page 4, lines 19-20 (supplement): If the detection efficiency for small particles was low, the peak shapes may be skewed. The possibility that similar peak shapes were obtained as a result of this bias needs to be discussed.

Author's Response: We agree with the referee's comment. There is a possibility that the peak shapes may be skewed due to the low detection efficiency for small particles (d_{va} < 0.2 μm). We noted that SSA-Aged, SSA-Bio and SSA-Ca exhibited similar size distribution, concentrating in size range of 0.4 - 0.7 μm and peaking around 0.5 μm, which indicated that SSA particles were aged during the inland transport and exhibited in fine particles. Besides, the transmission efficiencies of particles through the aerodynamic lens presented relative high in this size range (d_{va}) from 0.2 μm to 2 μm. (Fig. R1). Our results obtained were only based on this size (d_{va}) range. If the detection efficiency of small particles is improved, the peak shapes might skew. And the total peak shapes in size (d_{va}) range from 0.2 μm to 2 μm should also simultaneously skew. This change will little affect our present results. The following content is added:

“It is noted the results were only based on the size (d_{va}) range from 0.2 μm to 2 μm. There is a possibility that similar results were obtained for small particles ($d_{va} < 0.2$ μm).”

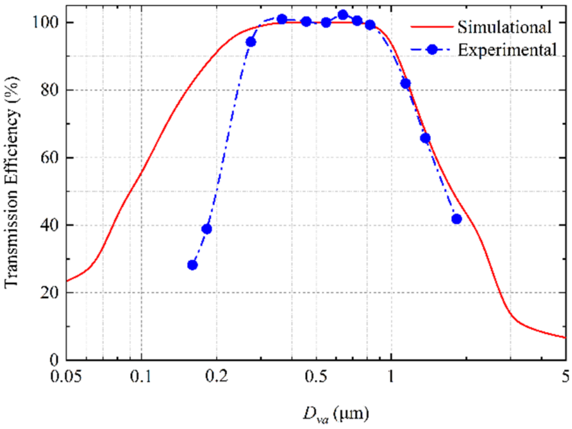

Figure R1. The simulational and experimental transmission efficiency of aerodynamic lens in SPAMS.

Technical corrections

R1-C24: Page 3, line 35: “may be associated”?

Author’s Response: Thanks for the technical suggestions. Revisions has been made accordingly.

Anonymous Referee #2

General comments

The manuscript presented the chemical composition of individual sea salt aerosol particles (SSA) using a single particle aerosol mass spectrometer (SPAMS). About 50,000 SSA from 2 million detected particles were identified. These SSA were classified as SSA-aged, SSA-bio, and SSA-Ca. The manuscript showed positive correlations between Na and organic acids. Thus, the authors claimed that organic acids played significant role in the chloride depletion, then up to 34% of depletion was estimated. It also claims that SSA-bio particles can be assigned as the biological origin. This study provides additional data sets for the better understanding in the atmospheric processes of sea salt aerosol. Some of the conclusions need clarifications before it can be considered for publication.

Author's Response: We appreciate the valuable time and efforts from the referee to improve the manuscript. Please see below for the point-by-point response to reviewers' comments.

Specific comments

R2-C1: Line 22, 321-323. Please clarify which part of the SSA-bio particles are biological origin? Do you mean the SSA part in SSA-bio particles, like [Na] detected in the mass spec. are these components also biological origin? If so, is there any previous studies showing that biological sources produces SSA-like particles or components? If not, that means among SSA, half of them are sea salt aerosol (likely from sea spray) mixed with biological components during the transport, then current statement is misleading and not accurate.

Author's Response: We agree with the reviewer's opinion that current statement is misleading and not accurate. In this study, three types of SSA particles with distinct mass spectral characteristics were obtained by using an Adaptive Resonance Theory neural network (ART-2a), including SSA-Aged, SSA-Bio and SSA-Ca. For SSA-Bio, it was identified not only by the general characteristics of the SSA (i.e., 23 $[Na]^+$, 46 $[Na_2]^+$, 62 $[Na_2O]^+$, 63 $[Na_2OH]^+$, 81 $[Na_2{}^{35}Cl]^+$ and 83 $[Na_2{}^{37}Cl]^+$), but also identified by the significant additional organic ion markers (e.g., amine (*m/z*: 58 $[C_2H_5NHCH_2]^+$ and 59 $[N(CH_3)_3]^+$), organic nitrogen (*m/z*: -26 $[CN]^-$ or 42 $[CNO]^-$) and phosphate (*m/z*: -63 $[PO_2]^-$, 79 $[PO_3]^-$)). This population of SSA with the above mentioned organic matters was identified as the "BioSS" in previous laboratory studies (Ault et al., 2014; Sultana et al., 2017). It is more likely produced by the ejection of SSA with microbes (e.g., phytoplankton and bacteria) in the sea surface microlayer (Cochran et al., 2017a; Cochran et al., 2017b; Wang et al., 2017). Thus, the mass spectra of SSA-Bio may be likely produced by the microbial, microbe-containing, or microbe-fragment-containing SSA particles, which is also similar with previous studies (Steele et al., 2003; Czerwieniec et al., 2005; Srivastava et al., 2005; Sultana et al., 2017).

We have rephrased this sentences as the summary of SSA-Bio particles as below:

"Ault et al. (2014) and Sultana et al. (2017) have also observed a special SSA type with higher biological ion markers in laboratory studies, which indicates it is more likely produced by the ejection of SSA with microbes (e.g., phytoplankton and bacteria) in SSML (Patterson et al., 2016; Cochran et al., 2017a; Cochran et al., 2017b; Wang et al., 2017)."

R2-C2: Line 23, 36-41, 251-252, 308-309. It is not clear how these conclusions were reached.

Author's Response:

Line 23: Organic acids considerably contribute to chloride depletion of SSA particles.

The results of strong correlation on hourly mean peak area between Na and organic acids and high number fraction of organic acids in SSA indicate the possible presence of organic salts in SSA and the substantial contribution of organic acids to the chloride depletion (Fig. 2 and Fig. 3). Additionally, the evaluation by relative peak area ratio also shows organic acids considerably contribute to chloride depletion of SSA particles.

Line 36-41: Strongly positive correlations between Na and organic acids (including formate, acetate, propionate, pyruvate, oxalate, malonate, succinate, and glutarate) were observed for the SSA-Aged ($r^2 = 0.52$, $p < 0.01$) and SSA-Bio ($r^2 = 0.61$, $p < 0.01$), indicating the significance of organic acids in the chloride depletion during inland transport.

In single particle mass spectrometry, the variation of peak area in time series could reveal the reaction mechanism of atmospheric chemistry (Zauscher et al., 2013). The correlation analysis based on peak area of different species could reflect the chemical composition of some types of particles in some content (Peng et al., 2019). Thus, we think that a perspective on correlation analysis between Na and organic acids may be likely to reflect the organic acids to chloride depletion.

Line 249-252: In the ageing process of the SSA particles, nitrate occupies a large proportion in the SSA-Aged (63-96%) and SSA-Bio particles (64-95%), respectively. Notably, chloride depletion attributed to organic acids could account for 2–34% in the SSA-Aged particles and 2–29% in the SSA-Bio particles.

The hourly mean relative peak area (RPA) ratio (acids / (sulfate + nitrate + organic acids)) is further applied to roughly evaluate the relative contribution of different acids (nitric acid, sulfuric acid, and organic acids) to the chloride depletion of SSA particles. The similar method was also introduced to evaluate the extent of chloride depletion in previous study (Ault et al., 2014). Further explanation cloud be seen in **R2-C3.**

Line 308-309: Up to 34% of chloride depletion could be explained by diverse organic acids.

The evaluation of acids to chloride depletion could be seen in **R2-C3.** We have reploted the Figure. S5 to exhibit the scale range of the relative contribution of acids to the chloride depletion in SSA particles. Based on this method, we think that up to 34% of chloride depletion could be explained by diverse organic acids.

R2-C3: Line 251-252, it claims organic acids contributed about 2-34% chloride depletion in SSA-aged, and 2-39% in SSA-bio particles. Where do these numbers come from? Are these estimates based on SPAMS or bulk measurements as showing in Line 270-276?

Author's Response: We used the data set via SPAMS of hourly mean relative peak area (RPA) ratio (i.e., acids / (sulfate + nitrate + organic acids)) to roughly evaluate the relative contribution of different acids to the chloride depletion of SSA particles. Each of hourly mean RPA ratio makes up the scale range of the relative contribution of acids to the chloride depletion in SSA particles. In order to further improve the reliability of this evaluation, we have referred the other citations as below:

"The similar method was also introduced to evaluate the extent of chloride depletion in previous study (Ault et al., 2014)."

R2-C4: In Fig.S5, organic acids only contribute less the 20% of all acids.

Author's Response: Thanks for the reviewer's opinion. We have also noticed the possibility of misleading from this part. We have reploted the Figure. S5 to exhibit the scale range of the relative contribution of acids to the chloride depletion in SSA particles.

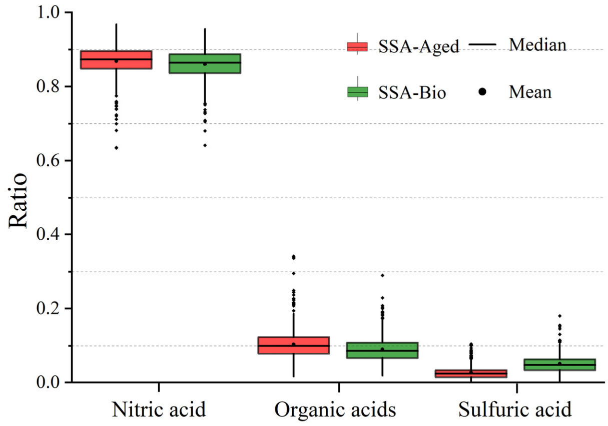

Figure S5. The relative contribution of different acids (nitric acid, sulfuric acid, and organic acids) to the chloride depletion of SSA particles. The ratio referred to the hourly mean relative peak area (RPA) ratio (acids / (sulfate + nitrate + organic acids)). Sulfate, nitrate and organic acids referred to peaks at *m/z* -97, *m/z* -46 and -62, and the mentioned organic acids in Fig. S4, respectively.

R2-C5: In Fig. 4 and Fig. 5, how can readers relate peak area of Cl/Na to the chloride depletion? For pure NaCl particles, what is the value of peak area of Cl/Na, if it is plotted in Fig.4/5?

Author's Response: Thanks for the reviewer's opinion. In order to improve the understanding for the broader readers, we have rephrased the figure caption of Figure. 4 and given the definition for Cl / Na in main text.

"Figure 4. A box and whisker plot of hourly mean peak area of Cl / Na in SSA-Aged and SSA-Bio. Herein, the Cl / Na value is applied to evaluate the ageing degree of SSA particles. There is a significant difference of Cl / Na between the SSA-Aged and SSA-Bio (1.9% versus 5.4%, by mean value, respectively). In the box and whisker plot, the lower and upper lines of the box denote the 25 and 75 percentiles, respectively. The lower and upper edges denote the 10 and 90 percentiles, respectively."

The definition of Cl/ Na is given in main text:

"In this study, Cl / Na value was defined as the ratio of hourly mean peak area of Cl to Na, which presented the degree of the chloride depletion in SSA particles."

For pure NaCl particles, we could hardly obtain the mass spectra because of the few responses of NaCl particles to 266 nm Nd:YAG laser with ca. 0.5 mJ laser energy. Briefly, there is a challenge for ionization and desorption of pure NaCl particles with the crystalline structure because of the disparity between the first ionization potentials of sodium (5.1 eV) and chlorine (13 eV) (Reents and Ge, 2000; Zawadowicz et al., 2015). If both easily ionized and difficult ionized species are simultaneously present, then charge will be transferred within the ion cloud from high-ionization-potential cations to neutral species having a low-ionization-potential (Reents and Schabel, 2001; Zawadowicz et al., 2015). Thus this, it is difficult to produce surface ionization for pure NaCl particles due to the relative high-ionization-potentials (Sinha and Friedlander, 1985, Hatch et al., 2011).

R2-C6: Line 288-291, the relation/trend shown in Fig. 5 does not mean that they are "direct evidence".

Author's Response: Thanks for the reviewer's opinion. We have deleted the "direct".

R2-C7: Line 270-276, please provide details for the bulk measurements.

Author's Response: Details for the bulk measurement and SPAMS analysis as shown below:

Sampling set names	Sampling dates	Duration (min)	Na^+	Ca^{2+}	Cl^-	NO_3^-	SO_4^{2-}	Cl^-% depletion	Peak area ratio of Cl / Na
Cloud Water 1	May 11	480	0.24	0.01	0.16	1.26	1.81	0.64	0.005*
Cloud Water 2	May 26	150	1.31	0.74	0.58	5.59	9.32	0.65	0.023
Cloud Water 3	May 26	140	1.73	0.98	0.56	3.90	6.48	0.74	0.028
Cloud Water 4	May 26	180	5.24	1.80	0.99	6.41	9.65	0.87	0.025
Cloud Water 5	May 27	214	1.98	1.21	1.08	9.33	13.84	0.55	0.029
Cloud Water 6	May 30	270	1.85	1.35	0.53	8.57	13.08	0.73	0.030
Cloud Water 7	May 30	305	1.88	1.07	0.79	11.14	16.95	0.67	0.028
Cloud Water 8	May 30	515	1.68	1.22	0.83	11.59	19.32	0.55	0.026
Cloud Water 9	Jun 1	225	1.07	0.79	0.31	5.57	5.71	0.73	0.028
Cloud Water 10	Jun 2	230	0.99	0.42	0.05	2.10	3.84	0.96	0.011
Cloud Water 11	Jun 2	141	1.63	0.59	0.30	3.84	5.64	0.88	0.016
Cloud Water 12	Jun 2	134	1.44	0.46	0.15	1.85	2.63	0.93	0.014
Cloud Water 13	Jun 2	203	3.79	1.03	0.35	3.85	5.80	0.94	0.046*
$PM_{2.5}$ 1	May 14-15	1440	1.12	1.04	0.38	1.05	2.60	0.62	0.038
$PM_{2.5}$ 2	May 18-19	1406	1.46	0.47	0.40	1.80	4.75	0.82	0.032
$PM_{2.5}$ 3	May 19-20	1423	0.45	0.22	0.07	2.07	5.09	0.88	0.031
$PM_{2.5}$ 4	May 20-21	1366	0.70	0.22	0.21	3.22	4.70	0.80	0.027
$PM_{2.5}$ 5	May 21-22	1431	0.48	0.18	0.13	2.11	3.52	0.82	0.029
$PM_{2.5}$ 6	May 22-23	1414	0.57	0.16	0.06	0.97	2.94	0.93	0.032
$PM_{2.5}$ 7	May 24-25	1419	0.72	0.21	0.17	2.59	4.22	0.80	0.054*
$PM_{2.5}$ 8	May 26-27	1391	0.72	0.47	0.25	2.36	3.20	0.70	0.029
$PM_{2.5}$ 9	May 29-30	1421	0.51	0.03	0.01	0.35	1.84	0.99	0.023
Mean			1.43	0.67	0.38	4.16	6.68	0.78	0.026

* These data are excluded because of the maximum (0.054), minimum (0.005) and abnomal value (0.046).

Table S1. The major ions, chloride depletion (%Cl^-) and hourly mean peak area ratio Cl / Na in the sample of cloud water and $PM_{2.5}$ during sampling period. The mass concentrations (μg m^{-3}) of Na^+, Ca^{2+}, Cl^-, NO_3^- and SO_4^{2-} were analyzed using an ion chromatography (Metrohm, Herisau, Switzerland). The cloud water was sampled by a Caltech Active Strand Cloud Water Collector Version 2 (CASCC2) (Modini et al., 2015), when visibility was < 3 km until the volume exceeded 250 ml. The PM2.5 was sampled using an Atmospheric particle sampler (Mingye Environmental Protection Technology Co., Ltd., China) with an inlet cyclone with a cut-off aerodynamic diameter of 2.5 μm.

In table S1, we simultaneously obtained the %Cl^- depletion and hourly mean peak area ratio Cl / Na corresponding to the sampling period. Then, we compared the degree of chloride depletion of SSA particles in quantitative analysis by mass concentration and semi-quantitative analysis by hourly mean peak area ratio.

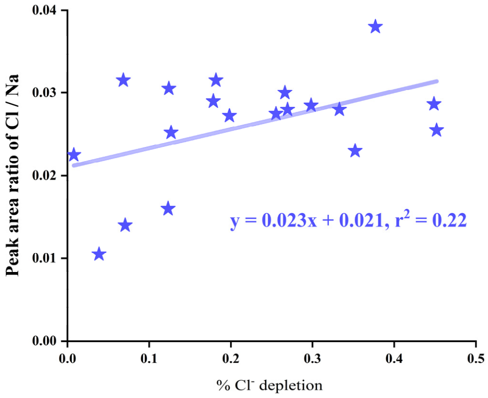

Fig S7. Correlation analysis of the both assessment methods of chloride depletion. These data were conducted significance test and $p < 0.001$. The correlation analysis was carried out on 19 among 22 set of data due to the rest of the maximum, minimum and the abnormal value (detailed in Table S1).

R2-C8: In the main text, please define "hourly mean peak area" in Figure 2 and "peak area of Cl/Na" (do you mean ratio of peak area of Cl to peak area of Na in y axis?) in Figure 4 and 5.

Author's Response: Thanks for the reviewer's opinion. We have given a definition for that.

"The linear correlations based on hourly mean peak area between Na and chloride, sulfate, nitrate, and organic acids in the SSA-Aged and SSA-Bio particles are shown in Fig. 2. Herein, hourly mean peak area was defined as the mean peak area of a component for hourly detected particles, indicating the variations of chemical composition in individual particles."

"In this study, Cl / Na value was defined as the ratio of hourly mean peak area of Cl to Na, which presented the degree of the chloride depletion in SSA particles."

R2-C9: Figure 3, what are the standard deviations in these numbers?

Author's Response: The number of individual particles was assumed to follow the Poisson distribution (Pratt et al., 2010; Lin et al., 2017), standard deviations for the hourly mean number fractions of major component in SSA-Aged and SSA-Bio as shown below:

Number fractions	Chloride	Sulfate	Organic acids	Nitrate	Ammonium	Amine	CN/CNO	Phosphate	C_2H_3	C_2H_3O
SSA-Aged	0.50	0.30	0.72	0.99	0.09	0.11	0.56	0.22	0.08	0.04
SSA-Bio	0.36	0.62	0.59	1.00	0.34	0.62	0.54	0.60	0.16	0.19

Standard deviations	Chloride	Sulfate	Organic acids	Nitrate	Ammonium	Amine	CN/CNO	Phosphate	C_2H_3	C_2H_3O
SSA-Aged	0.0045	0.0035	0.0054	0.0063	0.0019	0.0022	0.0048	0.0031	0.0018	0.0014
SSA-Bio	0.0039	0.0051	0.0050	0.0064	0.0038	0.0051	0.0047	0.0050	0.0026	0.0029

References

Ault, A. P., Guasco, T. L., Baltrusaitis, J., Ryder, O. S., Trueblood, J. V., Collins, D. B., Ruppel, M. J., Cuadra-Rodriguez, L. A., Prather, K. A., and Grassian, V. H.: Heterogeneous reactivity of nitric acid with nascent sea spray aerosol: Large differences observed between and within individual particles, J. Phys. Chem. Lett., 5, 2493-2500, http://doi.org/10.1021/jz5008802, 2014.

Braun, R. A., Dadashazar, H., MacDonald, A. B., Aldhaif, A. M., Maudlin, L. C., Crosbie, E., Aghdam, M. A., Hossein Mardi, A., and Sorooshian, A.: Impact of Wildfire Emissions on Chloride and Bromide Depletion in Marine Aerosol Particles, Environ. Sci. Technol., 51, 9013-9021, http://doi.org/10.1021/acs.est.7b02039, 2017.

Cai, Y., Zelenyuk., A., and Imre., D.: A High Resolution Study of the Effect of Morphology On the Mass Spectra of Single PSL Particles with Na-containing Layers and Nodules, Aerosol. Sci. Tech, 40, 1111–1122, http://doi.org/10.1080/02786820601001677, 2006.

Chi, J. W., Li, W. J., Zhang, D. Z., Zhang, J. C., Lin, Y. T., Shen, X. J., Sun, J. Y., Chen, J. M., Zhang, X. Y., Zhang, Y. M., and Wang, W. X.: Sea salt aerosols as a reactive surface for inorganic and organic acidic gases in the Arctic troposphere, Atmos. Chem. Phys., 15, 11341-11353, http://doi.org/10.5194/acp-15-11341-2015, 2015.

Chen, W., Wang, X., Cohen, J. B., Zhou, S., Zhang, Z., Chang, M., and Chan, C.-Y.: Properties of aerosols and formation mechanisms over southern China during the monsoon season, Atmos. Chem. Phys., 16, 13271-13289, http://doi.org/10.5194/acp-16-13271-2016, 2016.

Cochran, R. E., Laskina, O., Trueblood, J. V., Estillore, A. D., Morris, H. S., Jayarathne, T., Sultana, C. M., Lee, C., Lin, P., Laskin, J., Laskin, A., Dowling, J. A., Qin, Z., Cappa, C. D., Bertram, T. H., Tivanski, A. V., Stone, E. A., Prather, K. A., and Grassian, V. H.: Molecular Diversity of Sea Spray Aerosol Particles: Impact of Ocean Biology on Particle Composition and Hygroscopicity, Chem., 2, 655-667, http://doi.org/10.1016/j.chempr.2017.03.007, 2017a.

Cochran, R. E., Ryder, O. S., Grassian, V. H., and Prather, K. A.: Sea Spray Aerosol: The Chemical Link between the Oceans, Atmosphere, and Climate, Accounts Chem Res, 50, 599-604, http://doi.org/10.1021/acs.accounts.6b00603, 2017b.

Collins, D. B., Zhao, D. F., Ruppel, M. J., Laskina, O., Grandquist, J. R., Modini, R. L., Stokes, M. D., Russell, L. M., Bertram, T. H., Grassian, V. H., Deane, G. B., and Prather, K. A.: Direct aerosol chemical composition measurements to evaluate the physicochemical differences between controlled sea spray aerosol generation schemes, Atmos. Meas. Tech., 7, 3667-3683, http://doi.org/10.5194/amt-7-3667-2014, 2014.

Czerwieniec, G. A., Russell., S. C., Tobias., H. J., Pitesky., M. E., Fergenson., D. P., Steele., P., Srivastava., A., Horn., J. M., Frank., M., Gard., E. E., and Lebrilla., C. B.: Stable Isotope Labeling of Entire Bacillus atrophaeus Spores and Vegetative Cells Using Bioaerosol Mass Spectrometry, Anal. Chem. , 77, 1081-1087, http://doi.org/10.1021/ac0488098, 2005.

Dall'Osto, M., Harrison., R. M., and Beddows., D. c. S.: Single-Particle Detection Efficiencies of Aerosol Time-of-Flight Mass Spectrometry during the North Atlantic Marine Boundary Layer Experiment, Environ. Sci. Technol., 40, 5029-5035, http://doi.org/10.1021/es050951i, 2006.

Ghorai, S., Wang, B., Tivanski, A., and Laskin, A.: Hygroscopic properties of internally mixed particles composed of NaCl and water-soluble organic acids, Environ. Sci. Technol., 48, 2234-2241, http://doi.org/10.1021/es404727u, 2014.

Gross, D. S., Galli., M. E., Silva., P. J., and Prather., a. K. A.: Relative Sensitivity Factors for Alkali Metal and Ammonium Cations in Single-Particle Aerosol Time-of-Flight Mass Spectra, Anal. Chem., 72, 416-422, http://doi.org/10.1021/ac990434g, 2000.

Hatch, L. E., Creamean, J. M., Ault, A. P., Surratt, J. D., Chan, M. N., Seinfeld, J. H., Edgerton, E. S., Su, Y. X., and Prather, K. A.: Measurements of Isoprene-Derived Organosulfates in Ambient Aerosols by Aerosol Time-of-Flight Mass Spectrometry - Part 1: Single Particle Atmospheric Observations in Atlanta, Environ. Sci. Technol., 45, 5105-5111, http://doi.org/10.1021/es103944a, 2011.

Healy, R. M., Sciare, J., Poulain, L., Kamili, K., Merkel, M., Müller, T., Wiedensohler, A., Eckhardt, S., Stohl, A., Sarda-Estève, R., McGillicuddy, E., amp, apos, Connor, I. P., Sodeau, J. R., and Wenger, J. C.: Sources and mixing state of size-resolved elemental carbon particles in a European megacity: Paris, Atmos. Chem. Phys., 12, 1681-1700, http://doi.org/10.5194/acp-12-1681-2012, 2012.

Healy, R. M., Sciare, J., Poulain, L., Crippa, M., Wiedensohler, A., Prévôt, A. S. H., Baltensperger, U., Sarda-Estève, R., McGuire, M. L., Jeong, C. H., McGillicuddy, E., amp, apos, Connor, I. P., Sodeau, J. R., Evans, G. J., and Wenger, J. C.: Quantitative determination of carbonaceous particle mixing state in Paris using single-particle mass spectrometer and aerosol mass spectrometer measurements, Atmos. Chem. Phys., 13, 9479-9496, http://doi.org/10.5194/acp-13-9479-2013, 2013.

Hinz, K.-P., Trimborn, A., Weingartner, E., Henning, S., Baltensperger, U., and Spengler, B.: Aerosol single particle composition at the Jungfraujoch, J. Aerosol. Sci, 36, 123-145, http://doi.org/10.1016/j.jaerosci.2004.08.001, 2005.

Jeong, C. H., McGuire, M. L., Godri, K. J., Slowik, J. G., Rehbein, P. J. G., and Evans, G. J.: Quantification of aerosol chemical composition using continuous single particle measurements, Atmos. Chem. Phys., 11, 7027-7044, http://doi.org/10.5194/acp-11-7027-2011, 2011.

Kawamura, K., and Bikkina, S.: A review of dicarboxylic acids and related compounds in atmospheric aerosols: Molecular distributions, sources and transformation, Atmos. Res., 170, 140-160, http://doi.org/10.1016/j.atmosres.2015.11.018, 2016.

Lightowlers, P. J., and Cape, J. N.: Sources and fate of atmospheric HCl in the U.K. and western Europe, Atmos. Environ., 22, 7-15, http://doi.org/10.1016/0004-6981(88)90294-6, 1988.

Lin, Q, Yang, Y., Fu, Y., Zhang, G., Jiang, F., Peng, L., Lian, X., Liu, F., Bi, X., Li, L., Chen, D., Li, M., Ou, J., Tang, M., Wang, X., Peng, P., amp, apos, an, and Sheng, G.: Enrichment of submicron sea-salt-containing particles in small cloud droplets based on single-particle mass spectrometry, Atmos. Chem. Phys., 19, 10469-10479, http://doi.org/10.5194/acp-19-10469-2019, 2019.

Lin, Q, Yang, Y., Fu, Y., Jiang, F., Zhang, G., Peng, L., Lian, X., Bi, X., Li, L., Chen, D., Ou, J., Tang, M., Wang, X., Peng, P. a., and Sheng, G.: The reductions of oxalate and its precursors in cloud droplets relative to wet particles, Atmos. Environ., 235, http://doi.org/10.1016/j.atmosenv.2020.117632, 2020.

Lin, Q. H., Zhang, G. H., Peng, L., Bi, X. H., Wang, X. M., Brechtel, F. J., Li, M., Chen, D. H., Peng, P. A., Sheng, G. Y., and Zhou, Z.: In situ chemical composition measurement of individual cloud residue particles at a mountain site, southern China, Atmos. Chem. Phys., 17, 8473–8488, http://doi.org/10.5194/acp-17-8473-2017, 2017.

May, N. W., Gunsch, M. J., Olson, N. E., Bondy, A. L., Kirpes, R. M., Bertman, S. B., China, S., Laskin, A., Hopke, P. K., Ault, A. P., and Pratt, K. A.: Unexpected Contributions of Sea Spray and Lake Spray Aerosol to Inland Particulate Matter, Environ. Sci. Technol., 5, 405-412, http://doi.org/10.1021/acs.estlett.8b00254, 2018.

Modini, R. L., Frossard, A. A., Ahlm, L., Russell, L. M., Corrigan, C. E., Roberts, G. C., Hawkins, L. N., Schroder, J. C., Bertram, A. K., Zhao, R., Lee, A. K. Y., Abbatt, J. P. D., Lin, J., Nenes, A., Wang, Z., Wonaschütz, A., Sorooshian, A., Noone, K. J., Jonsson, H., Seinfeld, J. H., Toom-Sauntry, D., Macdonald, A. M.,and Leaitch, W. R.: Primary marine aerosol-cloud interactions off the coast of California, J. Geophys. Res., 120, 4282–4303, http://doi.org/10.1002/2014JD022963, 2015.

Patterson, J. P., Collins, D. B., Michaud, J. M., Axson, J. L., Sultana, C. M., Moser, T., Dommer, A. C., Conner, J., Grassian, V. H., Stokes, M. D., Deane, G. B., Evans, J. E., Burkart, M. D., Prather, K. A., and Gianneschi, N. C.: Sea Spray Aerosol Structure and Composition Using Cryogenic Transmission Electron Microscopy, ACS. Cent. Sci. , 2, 40-47, http://doi.org/10.1021/acscentsci.5b00344, 2016.

Peng, L., Li, L., Lin, Q., Li, M., Zhang, G., Bi, X., Wang, X., and Sheng, G.: Does atmospheric processing produce toxic Pb-containing compounds? A case study in suburban Beijing by single particle mass spectrometry, J. Hazard. Mater., 382, 121014, http://doi.org/10.1016/j.jhazmat.2019.121014, 2019.

Prather, K. A., Bertram, T. H., Grassian, V. H., Deane, G. B., Stokes, M. D., DeMott, P. J., Aluwihare, L. I., Palenik, B. P., Azam, F., Seinfeld, J. H., Moffet, R. C., Molina, M. J., Cappa, C. D., Geiger, F. M., Roberts, G. C., Russell, L. M., Ault, A. P., Baltrusaitis, J., Collins, D. B., Corrigan, C. E., Cuadra-Rodriguez, L. A., Ebben, C. J., Forestieri, S. D., Guasco, T. L., Hersey, S. P., Kim, M. J., Lambert, W. F., Modini, R. L., Mui, W., 545 Pedler, B. E., Ruppel, M. J., Ryder, O. S., Schoepp, N. G., Sullivan, R. C., and Zhao, D. F.: Bringing the ocean into the laboratory to probe the chemical complexity of sea spray aerosol, P. Natl. Acad. Sci. USA., 110, 7550-7555, http://doi.org/10.1073/pnas.1300262110, 2013.

Pratt, K. A., Heymsfield, A. J., Twohy, C. H., Murphy, S. M., DeMott, P. J., Hudson, J. G., Subramanian, R., Wang, Z. E., Seinfeld, J. H., and Prather, K. A.: In Situ Chemical Characterization of Aged Biomass-Burning Aerosols Impacting Cold Wave Clouds, J. Atmos. Sci., 67, 2451-2468, http://doi.org/10.1175/2010jas3330.1, 2010.

Pratt, K. A., and Prather, K. A.: Mass spectrometry of atmospheric aerosolsuRecent developments and applications. Part II: On-line mass spectrometry techniques, Mass. Spectrom. Rev., 31, 17-48, http://doi.org/10.1002/mas.20330, 2012.

Qin, X., Bhave., P. V., and Prather., K. A.: Comparison of Two Methods for Obtaining Quantitative Mass Concentrations from Aerosol Time-of-Flight Mass Spectrometry Measurements, Anal. Chem. , 78, 6169-6178, http://doi.org/10.1021/ac060395q, 2006.

Reents, W. D., and Ge, Z.: Simultaneous Elemental Composition and Size Distributions of Submicron Particles in Real Time Using Laser Atomization Ionization Mass Spectrometry, Aerosol. Sci. Tech., 33, 122-134, http://doi.org/10.1080/027868200410886, 2000.

Reents, W. D., and Schabel., M. J.: Measurement of Individual Particle Atomic Composition by Aerosol Mass Spectrometry, Anal. Chem. , 73, 5403-5414, http://doi.org/10.1021/ac010436c, 2001.

Sinha, M. P., and Friedlander., S. K.: Real-Time Measurement of Sodium Chloride in Individual Aerosol Particles by Mass Spectrometry, Anal. Chem., 57, 1880-1883, http://doi.org/10.1021/ac00286a019, 1985.

Song, X., and Hopke, P. K.: Classification of single particles analyzed by ATOFMS using an artificial neural network, ART-2A, Anal. Chem., 71, 860-865, http://doi.org/10.1021/ac9809682, 1999.

Srivastava, A., Pitesky., M. E., Steele., P. T., Tobias., H. J., Fergenson., D. P., Horn., J. M., Russell., S. C., Czerwieniec., G. A., Lebrilla., C. B., Gard., E. E., and Frank., M.: Comprehensive Assignment of Mass Spectral Signatures from Individual Bacillus atrophaeus Spores in Matrix-Free Laser Desorption/Ionization Bioaerosol Mass Spectrometry, Anal. Chem. , 77, 3315-3323, http://doi.org/10.1021/ac048298p, 2005.

Steele, P. T., Tobias., H. J., Fergenson., D. P., Pitesky., M. E., Horn., J. M., Czerwieniec., G. A., Russell., S. C., Lebrilla., C. B., Gard., E. E., and Frank., M.: Laser Power Dependence of Mass Spectral Signatures from Individual Bacterial Spores in Bioaerosol Mass Spectrometry, Anal. Chem. , 75, 5480-5487, http://doi.org/10.1021/ac034419u, 2003.

Sultana, C. M., Collins, D. B., and Prather, K. A.: Effect of Structural Heterogeneity in Chemical Composition on Online Single-Particle Mass Spectrometry Analysis of Sea Spray Aerosol Particles, Environ Sci Technol, 51, 3660-3668, http://doi.org/10.1021/acs.est.6b06399, 2017.

Trueblood, J. V., Estillore, A. D., Lee, C., Dowling, J. A., Prather, K. A., and Grassian, V. H.: Heterogeneous Chemistry of Lipopolysaccharides with Gas-Phase Nitric Acid: Reactive Sites and Reaction Pathways, J Phys Chem A, 120, 6444-6450, http://doi.org/10.1021/acs.jpca.6b07023, 2016.

Xiao, H.-s., Dong., J.-l., Wang., L.-y., Zhao., L.-j., Wang., F., and Zhang., Y.-h.: Spatially Resolved Micro-Raman Observation on the Phase Separation of Effloresced Sea Salt Droplets, Environ. Sci. Technol., 42, 8698–8702, http://doi.org/10.1021/es801181f, 2008.

Wang, B., and Laskin, A.: Reactions between water-soluble organic acids and nitrates in atmospheric aerosols: Recycling of nitric acid and formation of organic salts, J. Geophys. Res. Atmos., 119, 3335-3351, http://doi.org/10.1002/2013JD021169, 2014.

Wang, N., Lyu, X. P., Deng, X. J., Guo, H., Deng, T., Li, Y., Yin, C. Q., Li, F., and Wang, S. Q.: Assessment of regional air quality resulting from emission control in the Pearl River Delta region, southern China, Sci. Total. Environ., 573, 1554-1565, http://doi.org/10.1016/j.scitotenv.2016.09.013, 2016.

Wang, X. F., Deane, G. B., Moore, K. A., Ryder, O. S., Stokes, M. D., Beall, C. M., Collins, D. B., Santander, M. V., Burrows, S. M., Sultana, C. M., and Prather, K. A.: The role of jet and film drops in controlling the mixing state of submicron sea spray aerosol particles, P. Natl. Acad. Sci. USA, 114, 6978-6983, http://doi.org/10.1073/pnas.1702420114, 2017.

Wang, Y. Q.: MeteoInfo: GIS software for meteorological data visualization and analysis, Meteorol. Appl., 21, 360–368, https://doi.org/10.1002/met.1345, 2014.

Woods, E., Smith., G. D., Miller., R. E., and Baer., T.: Depth profiling of heterogeneously mixed aerosol particles using single-particle mass spectrometry, Anal. Chem. , 74, 1642-1649, http://doi.org/10.1021/ac0110909, 2002.

Wu, Z., Zhang, Y., Zhang, L., Huang, M., Zhong, L., Chen, D., and Wang, X.: Trends of outdoor air pollution and the impact on premature mortality in the Pearl River Delta region of southern China during 2006-2015, Sci. Total. Environ., 690, 248-260, http://doi.org/10.1016/j.scitotenv.2019.06.401, 2019.

Zauscher, M. D., Wang, Y., Moore, M. J. K., Gaston, C. J., and Prather, K. A.: Air Quality Impact and Physicochemical Aging of Biomass Burning Aerosols during the 2007 San Diego Wildfires, Environ Sci Technol, 47, 7633-7643, http://doi.org/10.1021/es4004137, 2013.

Zawadowicz, M. A., Abdelmonem, A., Mohr, C., Saathoff, H., Froyd, K. D., Murphy, D. M., Leisner, T., and Cziczo, D. J.: Single-Particle Time-of-Flight Mass Spectrometry Utilizing a Femtosecond Desorption and Ionization Laser, Anal. Chem., 87, 12221-12229, http://doi.org/10.1021/acs.analchem.5b03158, 2015.

Zelenyuk, A., Yang., J., Song., C., Zaveri., R. A., and Imre., D.: “Depth-Profiling” and Quantitative Characterization of the Size, Composition, Shape, Density, and Morphology of Fine Particles with SPLAT, a Single-Particle Mass Spectrometer, J. Phys. Chem. A 112, 669-677, http://doi.org/10.1021/jp077308y, 2008.

Zhang, G., Lian, X., Fu, Y., Lin, Q., Li, L., Song, W., Wang, Z., Tang, M., Chen, D., Bi, X., Wang, X., and Sheng, G.: High secondary formation of nitrogen-containing organics (NOCs) and its possible link to oxidized organics and ammonium, Atmos. Chem. Phys., 20, 1469-1481, http://doi.org/10.5194/acp-20-1469-2020, 2020.

Zhou, Y., Huang, X. H. H., Griffith, S. M., Li, M., Li, L., Zhou, Z., Wu, C., Meng, J., Chan, C. K., Louie, P. K. K., and Yu, J. Z.: A field measurement based scaling approach for quantification of major ions, organic carbon, and elemental carbon using a single particle aerosol mass spectrometer, Atmos. Environ., 143, 300-312, http://doi.org/10.1016/j.atmosenv.2016.08.054, 2016.

Impact of organic acids on chloride depletion of inland transported sea spray aerosols

Bojiang Su[1], Zeming Zhuo[1], Yuzhen Fu[2,3], Wei Sun[2,3], Ying Chen[1], Xubing Du[1], Yuxiang Yang[2,3],Si Wu[1], Fugui Huang[4], Duohong Chen[5], Lei Li[1,*], Guohua Zhang[2,6], Xinhui Bi[2,6], and Zhen Zhou[1]

[1] Guangdong Provincial Engineering Research Center for On-line Source Apportionment System of Air Pollution, Institute of Mass Spectrometry and Atmospheric Environment, Jinan University, Guangzhou 510632, PR China

[2] State Key Laboratory of Organic Geochemistry and Guangdong Key Laboratory of Environmental Protection and Resources Utilization, Guangzhou Institute of Geochemistry, Chinese Academy of Sciences, Guangzhou 510640, PR China

[3] University of Chinese Academy of Sciences, Beijing 100039, PR China

[4] Guangzhou Hexin Analytical Instrument Limited Company, Guangzhou 510530, PR China

[5] State Environmental Protection Key Laboratory of Regional Air Quality Monitoring, Guangdong Environmental Monitoring Center, Guangzhou 510308, PR China

[6] Guangdong-Hong Kong-Macao Joint Laboratory for Environmental Pollution and Control, Guangzhou Institute of Geochemistry, Chinese Academy of Sciences, Guangzhou 510640, PR China

Correspondence to: Lei Li (lileishdx@163.com)

Highlights

1. Half of the sea spray aerosol (SSA) particles could be assigned as the biological origin.
2. Organic acids considerably contribute to chloride depletion of SSA particles.
3. Biological organic coatings may inhibit heterogeneous reactions of SSA particles.

Abstract. Heterogeneous reactions on sea spray aerosols (SSA) are the potential pathway to drive the circulation of chlorine, nitrogen, and sulfur in the atmosphere. The release of Cl will significantly affect the physicochemical properties of SSA. However, the impact of organic acids and mixing state on chloride depletion of SSA is still unclear. Hence, the size and chemical composition of individual SSA particles during the East Asian summer monsoon were investigated by a single particle aerosol mass spectrometer (SPAMS). According to the chemical composition, SSA particles were classified into SSA-Aged, SSA-Bio and SSA-Ca. In comparison to the aged Na-rich SSA particles (SSA-Aged), some additional organic species related to biological origin were observed in SSA-Bio, and each of two types accounts for approximately 50% of total SSA particles. SSA-Ca may be associated with organic shell of Na-rich SSA particles, which only accounts for ~3%. Strongly positive correlations between Na and organic acids (including formate, acetate, propionate, pyruvate, oxalate, malonate, succinate, and glutarate) were observed for the SSA-Aged ($r^2 = 0.52$, $p < 0.01$) and SSA-Bio ($r^2 = 0.61$, $p < 0.01$), indicating the significance of organic acids in the chloride depletion during inland transport. The contribution of these organic acids to the chloride depletion is estimated to be up to 34%. Interestingly, the degree of chloride depletion is distinctly different between SSA-Aged and SSA-Bio. It is most probably attributed to the associated organic coating in the SSA-Bio particles, which inhibits the displacement reactions between acids and chloride. As revealed from the mixing state of SSA-Bio, Cl / Na ratio increases with increasing phosphate and organic nitrogen, which is known to originate from biological activities. This finding provides some basis for the improvement of modeling simulations in chlorine circulation and a comprehensive understanding of the effects of organics on chloride depletion of SSA particles.

Keywords:

Sea spray aerosols; individual particles; chloride depletion; mixing state; organic acids.

1 Introduction

As one of the largest natural sources of aerosols, sea spray aerosols (SSA) have a global flux of 2000-10000 Tg yr^{-1} (Gantt and Meskhidze, 2013) and global average distribution of 10.1 μg m^{-2} (Ma et al., 2008). SSA are highly complex mixtures, and the chemical composition and mixing state of original SSA depends on the components of local seawater and the mechanisms of formation (Wang et al., 2017). While fresh SSA particles contain approximately 90% sodium chloride (NaCl) in mass, multiphase reactions considerably affect the chemical composition and mixing state, and subsequently, the physical and chemical properties of SSA. The multiphase reactions of SSA, as have been widely reported in field experiments and laboratory studies (Ault et al., 2014; Ghorai et al., 2014; Ryder et al., 2015; Trueblood et al., 2016; Bondy et al., 2017; Martin et al., 2017; Bertram et al., 2018), drive the circulation of elements (e.g., C, O, N, S, P, Cl) affecting tropospheric chemistry and global ecosystem (Finlayson-Pitts, 2003).

As one of the most important reactions, chloride depletion, as shown in R1, in SSA by interacting with acidic species modifies the physicochemical properties of SSA.

$$\mathrm{HA}_{(g\ \mathrm{or}\ aq)} + \mathrm{NaCl}_{(aq\ \mathrm{or}\ s)} \rightarrow \mathrm{NaA}_{(aq\ \mathrm{or}\ s)} + \mathrm{HCl}_{(g\ \mathrm{or}\ aq)} \qquad \text{(R1)}$$

where NaCl represents the major component of SSA, and HA represents acidic species (e.g., HNO_3, H_2SO_4, and organic acids). Generally, inorganic acids are considered as the major contributors to chloride depletion in SSA (Dasgupta et al., 2007; Laskin et al., 2012; Chi et al., 2015), represented as:

HNO_3 (*g* or *aq*) + NaCl (*s* or *aq*) → $NaNO_3$ (*aq*) + HCl (*g* or *aq*) (R2)

H_2SO_4 (*g* or *aq*) + NaCl (*s* or *aq*) → Na_2SO_4 (*aq*) + HCl (*g* or *aq*) (R3)

However, growing evidence indicates that inorganic acids cannot fully explain the chloride depletion (Laskin et al., 2012). It is therefore proposed that organic acids should be included to further explain the mechanism of chlorine depletion in aged SSA (Ault et al., 2013; Wang and Laskin, 2014; Wang et al., 2015). Similarly, the heterogeneous reaction on SSA with organic acids can be described as (Wang and Laskin, 2014):

R-COOH (*g* or *aq*) + NaCl (*s* or *aq*) → R-COONa (*aq* or *s*) + HCl (*g* or *aq*) (R4)

R-COOH (*g* or *aq*) + $NaNO_3$ (*s* or *aq*) → R-COONa (*s* or *aq*) + HNO_3 (*g* or *aq*) (R5)

(*s*, solid; *aq*, aqueous; and *g*, gaseous)

The physicochemical properties of SSA could be substantially altered through the production of organic salts (Trueblood et al., 2016; Bertram et al., 2018). With ubiquitous existence in the atmosphere, some typical organic acids, such as formic acid, acetic acid, and oxalic acid, may potentially contribute to chloride depletion. Mochida et al. (2003) suggested that organic acids (e.g., oxalic acid and succinic acid) should be considered in the models in order to predict chloride depletion accurately. Through investigating the interactions between the pure NaCl and carboxylic acids in the laboratory, Laskin et al. (2012) even suggested interactions between carboxylic acids and NaCl was the main contribution of chloride depletion. Consistently, Ghorai et al. (2014) observed that some dicarboxylic acids might cause obvious chloride depletion under a specific meteorological condition. These dicarboxylic acids (e.g., malonic acid and succinic acid) are ubiquitous in urban and marine aerosols (Kawamura and Bikkina, 2016), which may come from the polluted continental outflow and the open ocean (Bikkina et al., 2015).

Given the potential contribution of organic acids to the chloride depletion, the understanding of the relative contribution and the influencing factors is still unclear. The investigation of factors that affect chloride depletion is indispensable to understand the ageing process of SSA and the ability to serve as cloud condensation nuclei (CCN) (Drozd et al., 2014; Wang et al., 2015). The morphology of fresh SSA particles is core-shell structure, which consists of salt-core dominated by sodium chloride and outer shell covered by K^+, Ca^{2+}, Mg^{2+}, SO_4^{2-}, Cl^- and organic components (Laskin et al., 2012; Collins et al., 2014; Chi et al., 2015). These organic components such as alkanes, fatty acids, sugars, dicarboxylic acids and phosphate may emitted from phytoplankton and bacteria in the sea surface microlayer (SSML) (Gaston et al., 2010; Bikkina et al., 2015; Cochran et al., 2017a; Cochran et al., 2017b; Wang et al., 2017), and the chemical composition and size distribution of SSA particles could be greatly changed by wave breaking. In recent literature, organic coatings on the particles resulted from atmospheric oxidation of hydrocarbons of biogenic and anthropogenic origin may significantly regulate uptake of N_2O_5 (Folkers et al., 2003; Ryder et al., 2014; Ryder et al., 2015).

In the present study, a single particle aerosol mass spectrometer (SPAMS) was used to investigate the particle size, chemical composition and ageing degree of individual SSA particles after long-range inland transport during the summer monsoon, to reveal the relative contribution of organic acids on chloride depletion and the influencing factors. The displacement reactions on the SSA particles with various types of organic acids are considered, and the results suggest a significant impact of organic acids on chloride depletion during inland transport. The influence of biogenic organics in the chloride depletion is also discussed.

2 Materials and Methods

2.1 Field site description

The sampling site is located at Nanling national background station (Mt. Tianjing, 24°41′56″ N, 112°53′56″ E; 1690 m a.s.l.), which was approximately 350 km north of the South China Sea and 200 km north of the Pearl River Delta (PRD) region. It is also surrounded by a national park forest (273 km^2), where there were barely anthropogenic pollutants. However, under the influence of the East Asian summer monsoon, the air mass originated from the South China Sea might cross the PRD region to the sampling site. As can be seen in *Supplement* Fig. S1, four major cluster back trajectories of air masses originated from the South China Sea and Indo China Peninsula transported across inland regions to the sampling site within 72 h. During the sampling period, the average relative humidity was 87%, the average temperature was 26.3°C, the wind direction was mainly southwesterly, and the average wind speed was 10 m s^{-1}. More detailed information on the meteorological data can be found in *Supplement* Fig. S2.

2.2 Instrumentation

Individual particles were analyzed using a SPAMS (Hexin Analytical Instrument Co., Ltd., China) from 11 May to 3 June 2018. The SPAMS was used to on-line measure the size and chemical composition of individual particles. The design and principles of SPAMS have been reported in detail previously (Li et al., 2011). Briefly, the aerosols are drawn into the aerodynamics lens. Then the collimated particles beam through two continuous laser beams (Nd: YAG laser, 532 nm) with a pace of 6 cm. The obtained time of flight and velocity are corresponding to the vacuum aerodynamic diameter. The velocity of an individual particle is applied to trigger the pulse laser (Nd: YAG laser, 266 nm). Subsequently, the generated ion fragments are detected by a bipolar time-of-flight mass spectrometer. Standard polystyrene latex spheres of 0.2-2.2 μm were used to calibrate vacuum aerodynamic particle sizes (d_{va}) of the measured individual particles.

Using single particle mass spectrometry (SPMS) alone is subjected to the transmission efficiencies of particles through the aerodynamic lens, the possible selectivity and matrix effects on chemical components, resulting in inaccuracies of the number concentration, size distribution and chemical composition of the ambient aerosols (Gross et al., 2000; Qin et al., 2006; Pratt and Prather, 2012). Thus, a comparison analysis based on the obtained particle counts, size distributions and peak area / relative peak area via SPMAS in this study should be considered as the semi-quantitative analysis from statistical perspective (Hinz et al., 2005; Jeong et al., 2011; Healy et al., 2012; Zhou et al., 2016). More detailed discussion for the semi-quantitative analysis of SSA particles could be seen in *Supplement*.

It is also noted that aerosols were sampled through two parallel inlets. The first one is a ground-based counterflow virtual impactor (GCVI model 1205, Brechtel Manufacturing Inc., USA), sampling the cloud residual particles, dried from cloud droplets (with size larger than 8 μm) during cloud event (i.e., when the relative humidity was higher than 95% and the visibility was lower than 3 km) (Zhang et al., 2017). The other one is a $PM_{2.5}$ sampling inlet, delivering fine particles during cloud-free periods. In the following discussion, the cloud residual particles and cloud-free particles were combined as the total of detected particles.

2.3 Classification of SSA

The general characteristic peaks of SSA particles include *m/z* 23 $[Na]^+$, 39 $[K]^+$, 46 $[Na_2]^+$, 62 $[Na_2O]^+$, 63 $[Na_2OH]^+$, 81 $[Na_2{}^{35}Cl]^+$ and 83 $[Na_2{}^{37}Cl]^+$ (Collins et al., 2014; Arndt et al., 2017; Martin et al., 2017). There are some additional organic peaks of biological origin (such as at *m/z* 58 $[C_2H_5NHCH_2]^+$, 59 $[N(CH_3)_3]^+$, 74 $[(C_2H_5)_2NH_2]^+$, -26 $[CN]^-$, -42 $[CNO]^-$, -63 $[PO_2]^-$, -79 $[PO_3]^-$, etc.), besides sodium-related peaks in SSA particles (Ault et al., 2014; Sultana et al., 2017b). In this study, SSA particles were identified by the presence of peaks at *m/z* 23, 46, 62, 63, 81 and 83, which was coincident with the previous study at the same site reported by Lin et al. (2019). In addition, these organic signals are also considerable for identification of SSA particles, when the above sodium related peaks exist.

A total of ~2 million detected particles were clustered into 8 groups using an

Adaptive Resonance Theory neural network (ART-2a) (Song and Hopke, 1999) with a vigilance factor of 0.75, a learning rate of 0.05 and a maximum of 20 iterations. In single particle mass spectral fingerprints, it is the key to distinguish SSA from other groups of particles whether to present the ion signature of 23 $[Na]^+$, 46 $[Na_2]^+$, 62 $[Na_2O]^+$, 63 $[Na_2OH]^+$, 81 $[Na_2{}^{35}Cl]^+$ and 83 $[Na_2{}^{37}Cl]^+$ simultaneously (Ault et al., 2014; Collins et al., 2014; Lin et al., 2019). Based on the above representative peaks, ~50 000 SSA particles were identified. Three types of SSA particles with distinct mass spectral characteristics were obtained, including ~25 000 SSA-Aged, ~25 000 SSA-Bio and 1 500 SSA-Ca, respectively. We note that the mass spectral characteristics of SSA for the cloud residual particles ensemble those for the cloud-free particles. And therefore, we focus on the influence of long-range transport, rather than in-cloud process, on the modification of SSA.

3. Results and discussion

3.1 General characteristics of inland transported SSA particles

Figure 1 provides the averaged positive and negative ion mass spectra of three types of SSA particles. SSA-Aged is characterized by prominent ion signature for *m/z* at 23 $[Na]^+$, 39 $[K]^+$, 40 $[Ca]^+$, 46 $[Na_2]^+$, 62 $[Na_2O]^+$ and 63 $[Na_2OH]^+$. Some contributions from *m/z* 24 $[Mg]^+$, 56 $[Fe]^+$ or 56 $[CaO]^+$, 81 $[Na_2{}^{35}Cl]^+$, 83 $[Na_2{}^{37}Cl]^+$, 108 $[Na_2NO_3]^+$ and 165 $[Na_2SO_4]^+$ were also observed. These mass spectral characteristics are similar to those in previous literature (Hughes et al., 2000; Collins et al., 2014; Sultana et al., 2017a). This type of SSA particles with a significant ion marker of Na is typically represented as Na-rich sea salt particles. In the negative ion spectra, abundant nitrate were observed due to the ratio of *m/z* at -46 $[NO_2]^-$, -62 $[NO_3]^-$, and -147 $[Na(NO_3)_2]^-$, in contrast to weak chlorine ion signal at *m/z* -35 $[^{35}Cl]^-$ and -37 $[^{37}Cl]^-$, indicating that the particles have undergone partial but not fully atmospheric ageing (Hughes et al., 2000; Sultana et al., 2017b). Several peaks are assigned as organic acids, such as formate at *m/z* -45 $[HCO_2]^-$, acetate at *m/z* -59 $[C_2H_3O_2]^-$, propionate at *m/z* -73 $[C_2HO_3]^-$, pyruvate at *m/z* -87 $[C_3H_3O_3]^-$, oxalate at *m/z* -89 $[C_2HO_4]^-$, malonate at *m/z* -103 $[C_3H_3O_4]^-$, succinate at *m/z* -117 $[C_4H_5O_4]^-$, and glutarte at *m/z* -131 $[C_5H_7O_4]^-$ (Lin et al., 2019), which may be related to algal activity in the SSML or conversion of second organic aerosols (SOAs) in the atmosphere (O'Dowd et al., 2014).

Compared with SSA-Aged, the averaged ion spectra of SSA-Bio are more complex. SSA-Bio had significant additional signals from biological organic matter (i.e., organic nitrogen and phosphate), besides the general characteristics of the SSA-Aged particles (Prather et al., 2013; Ault et al., 2014; Guasco et al., 2014). While these markers might also be associated with dust (Zawadowicz et al., 2017), it is most likely attributed to biological markers herein, since there is negligible ion marker (e.g., Al, Ti, Si) for dust. Distinct characteristics of amines (58 $[C_2H_5NHCH_2]^+$, 59 $[N(CH_3)_3]^+$) were presented in the positive spectra, which is similar to the results in a prior laboratory study (Ault et al., 2014; Sultana et al., 2017a). Besides, the source of amines could also be influenced by the formation of secondary species (such as animal husbandry and biomass burning) during transport (Cheng et al., 2018). The organic nitrogen (i.e., -26 $[CN]^-$, -42 $[CNO]^-$) has been assigned to the ionization of amino acids in previous studies (Srivastava et al., 2005; Czerwieniec. et al., 2005). Phosphate peaks at *m/z* -63 $[PO_2]^-$ and -79 $[PO_3]^-$ are likely assigned as the ionization of components such as phospholipids in biological cells (Fergenson, 2004; Collins et al., 2013; Cochran et al., 2017a; Cochran et al., 2017b; Nguyen et al., 2017). It is noted that SSA-Bio should be regarded as the SSA population influenced by biological activity (Prather et al., 2013). In addition, the peaks of *m/z* 56 represents $[CaO]^+$ / $[KOH]^+$ or $[^{56}Fe]^+$. In contrast to SSA-Aged, those aforementioned organic acids exhibited higher peak signal in SSA-Bio. Similar to SSA-Aged, inorganic acids (-46 $[NO_2]^-$, -62 $[NO_3]^-$ and -97 $[HSO_4]^-$) with strong ion signals were also observed. Despite of the different mass spectral pattern, the behavior and inland transport of SSA-Aged and SSA-Bio may be similar. As can be seen in Fig. S1, the relative proportions of them keep stable in the different air masses. They also exhibit similar size distribution, concentrating in size range of 0.4-0.7 μm and peaking around 0.5 μm (Fig. S3).

SSA-Ca is identified by relatively higher contributions from calcium-related compounds at *m/z* 40 $[Ca]^+$, 56 $[CaO]^+$, 57 $[CaOH]^+$, 75 $[Ca^{35}Cl_2]^+$, 77 $[Ca^{37}Cl_2]^+$, and 113 $[(CaO)_2H]^+$, whereas associated with smaller sodium peak than other types. The negative spectra are dominated by nitrate, sulfate, organic nitrogen, phosphate and chloride. This SSA population has been previously classified as “organic-carbon-dominated (OC)” (Prather et al., 2013; Collins et al., 2014), likely resulted from the coating of Na-rich SSA particles through crystallization and precipitation of Ca-containing sulfate (e.g., calcium sulfate and sodium calcium sulfate) during the dehydration of sea water and seawater droplets (Xiao et al., 2008; Sultana et al., 2017b;

May et al., 2018). The mass spectral characteristics of the Ca-rich SSA particles are quite similar to those of lake spray aerosols (Axson et al., 2016; May et al., 2018). However, SSA-Ca only accounts for a negligible fraction (3.2%) and thus will not be covered in the following discussions.

3.2 Contribution of organic acids to the chloride depletion in the SSA particles

The linear correlations based on hourly mean peak area between Na and chloride, sulfate, nitrate, and organic acids in the SSA-Aged and SSA-Bio particles are shown in Fig. 2. Herein, hourly mean peak area was defined as the mean peak area of a component for hourly detected particles, indicating the variations of chemical composition in individual particles. As expected, there are strong correlations between Na and nitrate in both the SSA-Aged ($r^2 = 0.79$, $p < 0.01$) and SSA-Bio ($r^2 = 0.86$, $p < 0.01$) particles. In addition, more than 99% of SSA particles are internally mixed with nitrate (Fig. 3). This indicates that chemistry in Reaction 2 (R2) is prevalent during long-range transport (Bondy et al., 2017). This is also consistent with previous studies regarding that nitric acid is a major contributor to chloride depletion (Zhao and Gao, 2008; Chi et al., 2015; AzadiAghdam et al., 2019). It is possible supported by the relative high concentration of its precursor NO_x (4.67 μg m^{-3}) in the south China sector (Wang et al., 2016; Wu et al., 2019).

Strong positive correlations between Na and organic acids are also observed in both the SSA-Aged ($r^2 = 0.52$, $p < 0.01$) and SSA-Bio particles ($r^2 = 0.61$, $p < 0.01$). Furthermore, very high number fractions (NFs) of organic acids are also found in SSA-

Aged (72%) and SSA-Bio (59%), as shown in Fig. 3. This indicates the possible presence of organic salts in SSA particles and the substantial contribution of organic acids to the chloride depletion. The detailed mixing state (by NFs) between SSA particles and several detected organic acids, as shown in Fig. S4, indicates that formate, oxalate, malonate, and glutarate are the dominant salts. This result may be associated with the wide range of occurrence of corresponding organic acids in the atmosphere (Ghorai et al., 2014; Kawamura and Bikkina, 2016). The hourly mean relative peak area (RPA) ratio (acids / (sulfate + nitrate + organic acids)) is further applied to roughly evaluate the relative contribution of different acids (nitric acid, sulfuric acid, and organic acids) to the chloride depletion of SSA particles (Fig. S5). The similar method was also introduced to evaluate the extent of chloride depletion in previous study (Ault et al., 2014). In the ageing process of the SSA particles, nitrate occupies a large proportion in the SSA-Aged (63-96%) and SSA-Bio particles (64-95%), respectively. Notably, chloride depletion attributed to organic acids could account for 2–34% in the SSA-Aged particles and 2–29% in the SSA-Bio particles. The relative contribution of organic acids to chloride depletion has been reported to be higher than 30% at the eastern United States coast (Braun et al., 2017) and up to 40% in Southeast Asia (AzadiAghdam et al., 2019). The contribution of sulfuric acids (0-10% versus 0-18 %) is the lowest, although it shows positive correlation ($r^2 = 0.24$, $p < 0.01$ versus $r^2 = 0.54$, $p < 0.01$) for the SSA-Aged and SSA-Bio particles, respectively (Fig. 2). In addition, similar variations in hourly mean peak area of sulfate, nitrate and organic acids were observed in the SSA-Aged and SSA-Bio particles throughout the sampling period (Fig.

S6), indicating a close connection of the formation mechanism between inorganic and organic acids.

3.3 Effect of particle type on chloride depletion

Cl / Na value is typically applied to evaluate the ageing degree of SSA particles (Laskin et al., 2012; Bondy et al., 2017). In this study, Cl / Na value was defined as the ratio of hourly mean peak area of Cl to Na, which presented the degree of the chloride depletion in SSA particles. There is a significant difference of Cl / Na between the SSA-Aged (1.9%) and SSA-Bio (5.4%) particles (Fig. 4). This result reflects less chloride remaining in the SSA-Aged, attributed to more severe ageing. It might also be supported by relatively weak positive correlation ($r^2 = 0.46$, $p < 0.01$) between Na and Cl (Fig. 2). This result may be explained by the influence of chemical composition and mixing state on the evolution of the SSA particles (Collins et al., 2014; Quinn et al., 2015; Sultana et al., 2017b). Additionally, concentration calculation was also further quantified the chloride depletion percentage using the following equation:

$$\%Cl^- \text{ depletion} = (1.81 \times [Na^+] - [Cl^-]) / (1.81 \times [Na^+]) \times 100\% \qquad (R6)$$

where $[Na^+]$ and $[Cl^-]$ are mass concentrations ($\mu g\ m^{-3}$), and 1.81 is the typical mass ratio of Cl / Na in seawater (Zhao and Gao, 2008; Braun et al., 2017; AzadiAghdam et al., 2019). The mass concentration of major ions (such as Na^+ and Cl^-) was analyzed using an ion chromatography (Metrohm, Herisau, Switzerland), detailed information could be found in *supplement* Table S1. The overall $\%Cl^-$ for the total SSA particles varying from 55% to 99% with an average of 78% (Table S1), which is similar to the previous field study in the PRD region reported by Chen et al. (2016). However, SSA particles are not the only source of chlorine ion in the atmosphere (Lightowlers et al., 1988). It is noted that excess $[Cl]^-$ produced by fuel combustion (Lightowlers et al., 1988) could lower the $\%Cl^-$ and high sensitivity of SPAMS to Na^+ (Gross et al., 2000) could increase the Cl / Na value. These potential inaccuracies might be more likely to explain the weak difference for the two assessment methods of ageing degree of SSA particles, which are evaluated by hourly mean peak area of Cl / Na and quantification of chloride depletion on mass concentration. Generally, the quantitative analysis of mass concentration could directly evaluate the degree of chloride depletion in SSA particles (Braun et al., 2017). We note that there are some consistencies between the two assessment methods, which are supported by a positive correlation ($r^2 = 0.22$, $p < 0.001$) (Fig. S7). Hence, the hourly mean peak area of Cl / Na could also semi – quantitatively reflect the degree of chloride depletion, in some extent.

Further analysis indicates that organic matter of biological origin might play an important role in such inhibition of chloride depletion in the SSA-Bio particles. It is supported by the relationship between hourly mean peak area ratio of Cl / Na and the biological origin markers (-26 $[CN]^-$, -42 $[CNO]^-$, -63 $[PO_2]^-$ and -79 $[PO_3]^-$) described in section 3.1. As shown in Fig. 5, hourly mean peak area ratio of Cl / Na exhibits an increasing trend with both phosphate (-63 $[PO_2]^-$, -79 $[PO_3]^-$) and organic nitrogen (-26 $[CN]^-$ and -42 $[CNO]^-$). This evidence indicated phosphate might have a considerable effect on chloride depletion in SSA particles. The relationship between Cl / Na and organic nitrogen is also consistent with that reported in our previous field observations at the same site (Lin et al., 2019). Previous laboratory study results have also shown that reactivity could be inhibited by the organic matter of biological origin (Ault et al., 2014; Ryder et al., 2015). As shown in Fig. S8, transmission electron microscopy (TEM) images clearly show NaCl core and organic coating of the SSA particles with various thicknesses. The thicker organic coating may inhibit the reactive uptake of HNO_3 $_{(g)}$ or N_2O_5 $_{(g)}$ to SSA particles (Folkers et al., 2003; Ryder et al., 2014; Ryder et al., 2015), resulting in a less released Cl to the atmosphere. Such organic coatings are mostly composed of long-chain hydrocarbon, saccharides, carbohydrate, amine and anionic surfactant (Jayarathne et al., 2016; Bertram et al., 2018), and thus have stronger hydrophobicity and probably inhibit the occurrence of Cl transport of convection and diffusion (Bondy et al., 2017).

4. Conclusion and atmospheric implication

We investigated the chloride depletion of SSA particles after long-range inland transport in south China, during a monsoon season. The SSA particles still account for ~3% of the observed submicron particles and are extensively internally mixed with various acids. While the contribution of nitric acid dominates over other acids to the chloride depletion, our results suggest that the role of organic acids should not be neglected. Up to 34% of chloride depletion could be explained by diverse organic acids. Our results add to the growing body of evidence that carboxylic acid may play a significant role in acid displacement reactions (Ma et al., 2013). Given the substantial influence of organic acids on the hygroscopic properties of SSA (Ghorai et al., 2014), such processes may affect CCN / IN activities and lifetime of SSA (Knopf et al., 2014), and thus should be considered in models to predict the climate impact of SSA accurately. Currently, the calculation model of organic acids (especially water-soluble organic compounds) to chloride depletion is still limited (Laskin et al., 2012; Xu et al., 2013). Peng et al. (2016) suggested organic salts produced by NaCl react with dicarboxylic acids inhibit the volatilization of HCl that is resulting in less chloride depletion. Our data may improve the understanding of chloride depletion responsible for mixing state of diverse organic acids in the future study.

In addition, this is the first report to observe the SSA type of biological orgin in field study. Ault et al. (2014) and Sultana et al. (2017a) have also observed a special SSA type with higher biological ion markers in laboratory studies, which indicates it is more likely produced by the ejection of SSA with microbes (e.g., phytoplankton and bacteria) in the SSML (Patterson et al., 2016; Cochran et al., 2017a; Cochran et al., 2017b; Wang et al., 2017). We stress that there is a SSA type (i.e., SSA-Bio) likely attributed to the biological origin, exhibiting distinctly different chloride depletion, in comparison with the commonly observed SSA-Aged type. Our data indicate that organic matter of biological origin might play an essential role in such inhibition of chloride depletion in the SSA-Bio particles. As previously reported, the presence of organic coatings on SSA particles could effectively influence the heterogeneous reactivity of SSA particles (Ryder et al., 2015; Bondy et al., 2017). Considering the considerable contribution (~50%) of the SSA-Bio particles to the overall SSA, such information should be useful to improve that model results for the climate impact of

SSA.

Author contributions

GHZ, LL, and XHB designed the research. BJS, GHZ, and LL analyzed the data, and wrote the manuscript. YZF, XBD, YC, YXY and WS conducted sampling work under the guidance of GHZ, LL, and XHB. DHC had an active role in supporting the sampling work. YZF performed the laboratory analysis of individual particles by TEM/EDS. All authors contributed to the discussions of the results and refinement of the manuscript.

Data availability. Data are available on request from Lei Li (lileishdx@163.com).

Acknowledgement

This work was supported by the National Nature Science Foundation of China (No. 41905106), Guangdong International Science and Technology Cooperation Project (2018A050506020) and Guangdong Foundation for Program of Science and Technology Research (Grant No. 2019B121205006).

Competing interests. The authors declare that they have no conflict of interest.

References

Arndt, J., Sciare, J., Mallet, M., Roberts, G. C., Marchand, N., Sartelet, K., Sellegri, K., Dulac, F., Healy, R. M., and Wenger, J. C.: Sources and mixing state of summertime background aerosol in the north-western Mediterranean basin, Atmos. Chem. Phys, 17, 6975-7001, http://doi.org/10.5194/acp-17-6975-2017, 2017.

Ault, A. P., Moffet, R. C., Baltrusaitis, J., Collins, D. B., Ruppel, M. J., Cuadra-Rodriguez, L. A., Zhao, D. F., Guasco, T. L., Ebben, C. J., Geiger, F. M., Bertram, T. H., Prather, K. A., and Grassian, V. H.: Size-Dependent Changes in Sea Spray Aerosol Composition and Properties with Different Seawater Conditions, Environ. Sci. Technol., 47, 5603-5612, http://doi.org/10.1021/es400416g, 2013.

Ault, A. P., Guasco, T. L., Baltrusaitis, J., Ryder, O. S., Trueblood, J. V., Collins, D. B., Ruppel, M. J., Cuadra-Rodriguez, L. A., Prather, K. A., and Grassian, V. H.: Heterogeneous reactivity of nitric acid with nascent sea spray aerosol: Large differences observed between and within individual particles, J. Phys. Chem. Lett., 5, 2493-2500, http://doi.org/10.1021/jz5008802, 2014.

Axson, J. L., May, N. W., Colon-Bernal, I. D., Pratt, K. A., and Ault, A. P.: Lake Spray Aerosol: A Chemical Signature from Individual Ambient Particles, Environ. Sci. Technol., 50, 9835-9845, http://doi.org/10.1021/acs.est.6b01661, 2016.

AzadiAghdam, M., Braun, R. A., Edwards, E.-L., Bañaga, P. A., Cruz, M. T., Betito, G., Cambaliza, M. O., Dadashazar, H., Lorenzo, G. R., Ma, L., MacDonald, A. B., Nguyen, P., Simpas, J. B., Stahl, C., and Sorooshian, A.: On the nature of sea salt aerosol at a coastal megacity: Insights from Manila, Philippines in

Southeast Asia, Atmos. Environ., 216, http://doi.org/10.1016/j.atmosenv.2019.116922, 2019.

Bertram, T. H., Cochran, R. E., Grassian, V. H., and Stone, E. A.: Sea spray aerosol chemical composition: elemental and molecular mimics for laboratory studies of heterogeneous and multiphase reactions, Chem. Soc. Rev., 47, 2374-2400, http://doi.org/10.1039/c7cs00008a, 2018.

Bikkina, S., Kawamura, K., and Miyazaki, Y.: Latitudinal distributions of atmospheric dicarboxylic acids, oxocarboxylic acids, andα-dicarbonyls over the western North Pacific: Sources and formation pathways, J. Geophys. Res. Atmos., 120, 5010-5035, http://doi.org/10.1002/2014jd022235, 2015.

Bondy, A. L., Wang, B., Laskin, A., Craig, R. L., Nhliziyo, M. V., Bertman, S. B., Pratt, K. A., Shepson, P. B., and Ault, A. P.: Inland sea spray aerosol transport and incomplete chloride depletion: Varying degrees of reactive processing observed during soas, Environ. Sci. Technol., 51, 9533-9542, http://doi.org/10.1021/acs.est.7b02085, 2017.

Braun, R. A., Dadashazar, H., MacDonald, A. B., Aldhaif, A. M., Maudlin, L. C., Crosbie, E., Aghdam, M. A., Hossein Mardi, A., and Sorooshian, A.: Impact of Wildfire Emissions on Chloride and Bromide Depletion in Marine Aerosol Particles, Environ. Sci. Technol., 51, 9013-9021, http://doi.org/10.1021/acs.est.7b02039, 2017.

Chen, W., Wang, X., Cohen, J. B., Zhou, S., Zhang, Z., Chang, M., and Chan, C.-Y.: Properties of aerosols and formation mechanisms over southern China during the monsoon season, Atmos. Chem. Phys., 16, 13271-13289, http://doi.org/10.5194/acp-16-13271-2016, 2016.

Cheng, C., Huang, Z., Chan, C. K., Chu, Y., Li, M., Zhang, T., Ou, Y., Chen, D., Cheng, P., Li, L., Gao, W., Huang, Z., Huang, B., Fu, Z., and Zhou, Z.: Characteristics and mixing state of amine-containing particles at a rural site in the Pearl River Delta, China, Atmos. Chem. Phys., 18, 9147-9159, http://doi.org/10.5194/acp-18-9147-2018, 2018.

Chi, J. W., Li, W. J., Zhang, D. Z., Zhang, J. C., Lin, Y. T., Shen, X. J., Sun, J. Y., Chen, J. M., Zhang, X. Y., Zhang, Y. M., and Wang, W. X.: Sea salt aerosols as a reactive surface for inorganic and organic acidic gases in the Arctic troposphere, Atmos. Chem. Phys., 15, 11341-11353, http://doi.org/10.5194/acp-15-11341-2015, 2015.

Cochran, R. E., Laskina, O., Trueblood, J. V., Estillore, A. D., Morris, H. S., Jayarathne, T., Sultana, C. M., Lee, C., Lin, P., Laskin, J., Laskin, A., Dowling, J. A., Qin, Z., Cappa, C. D., Bertram, T. H., Tivanski, A. V., Stone, E. A., Prather, K. A., and Grassian, V. H.: Molecular Diversity of Sea Spray Aerosol Particles: Impact of Ocean Biology on Particle Composition and Hygroscopicity, Chem., 2, 655-667, http://doi.org/10.1016/j.chempr.2017.03.007, 2017a.

Cochran, R. E., Ryder, O. S., Grassian, V. H., and Prather, K. A.: Sea Spray Aerosol: The Chemical Link between the Oceans, Atmosphere, and Climate, Acc. Chem. Res., 50, 599-604, http://doi.org/10.1021/acs.accounts.6b00603, 2017b.

Collins, D. B., Ault, A. P., Moffet, R. C., Ruppel, M. J., Cuadra-Rodriguez, L. A., Guasco, T. L., Corrigan, C. E., Pedler, B. E., Azam, F., Aluwihare, L. I., Bertram, T. H., Roberts, G. C., Grassian, V. H., and Prather, K. A.: Impact of marine biogeochemistry on the chemical mixing state and cloud forming ability of nascent sea spray aerosol, J. Geophys. Res. Atmos., 118, 8553-8565, http://doi.org/10.1002/jgrd.50598, 2013.

Collins, D. B., Zhao, D. F., Ruppel, M. J., Laskina, O., Grandquist, J. R., Modini, R. L., Stokes, M. D., Russell, L. M., Bertram, T. H., Grassian, V. H., Deane, G. B., and Prather, K. A.: Direct aerosol chemical composition measurements to evaluate the physicochemical differences between controlled sea spray aerosol generation schemes, Atmos. Meas. Tech., 7, 3667-3683, http://doi.org/10.5194/amt-7-3667-2014, 2014.

Czerwieniec., G. A., Russell., S. C., Tobias., H. J., Pitesky., M. E., Fergenson., D. P., Steele., P., Srivastava., A., Horn., J. M., Frank., M., Gard., E. E., and Lebrilla., C. B.: Stable Isotope Labeling of Entire Bacillus atrophaeus Spores and Vegetative Cells Using Bioaerosol Mass Spectrometry, Anal. Chem., 77, 1081-1087, http://doi.org/10.1021/ac0488098, 2005.

Dasgupta, P. K., Campbell, S. W., Al-Horr, R. S., Ullah, S. M. R., Li, J., Amalfitano, C., and Poor, N. D.: Conversion of sea salt aerosol to NaNO3 and the production of HCl: Analysis of temporal behavior of aerosol chloride/nitrate and gaseous HCl/HNO3 concentrations with AIM, Atmos. Environ., 41, 4242-4257, http://doi.org/10.1016/j.atmosenv.2006.09.054, 2007.

Drozd, G., Woo, J., Häkkinen, S. A. K., Nenes, A., and McNeill, V. F.: Inorganic salts interact with oxalic acid in submicron particles to form material with low hygroscopicity and volatility, Atmos. Chem. Phys., 14, 5205-5215, http://doi.org/10.5194/acp-14-5205-2014, 2014.

Fergenson, P. D. M. E. P., Herbert J. Tobias, Paul T. Steele, Gregg A. Czerwieniec, Scott C. Russell, Carlito B. Lebrilla, Joanne M. Horn, Keith R. Coffee, Abneesh Srivastava, Segaran P. Pillai, Meng-Ta Peter Shih, Howard L. Hall, Albert J. Ramponi, John T. Chang, Richard G. Langlois, Pedro L. Estacio, Robert T. Hadley, Matthias Frank, and Eric E. Gard*,: Reagentless Detection and Classification of Individual Bioaerosol Particles in Seconds, Anal. Chem., 76, 373-378, http://doi.org/10.1021/ac034467e, 2004.

Finlayson-Pitts, B. J.: The tropospheric chemistry of sea salt: A molecular-level view of the chemistry of nacl and nabr, Chem. Rev. , 103, 4801−4822, http://doi.org/10.1021/cr020653t, 2003.

Folkers, M., Mentel, T. F., and Wahner, A.: Influence of an organic coating on the reactivity of aqueous aerosols probed by the heterogeneous hydrolysis of N2O5, Geophys. Res. Lett., 30, http://doi.org/10.1029/2003gl017168, 2003.

Gantt, B., and Meskhidze, N.: The physical and chemical characteristics of marine primary organic aerosol: a review, Atmos. Chem. Phys., 13, 3979-3996, http://doi.org/10.5194/acp-13-3979-2013, 2013.

Gaston, C. J., Pratt, K. A., Qin, X. Y., and Prather, K. A.: Real-Time Detection and Mixing State of Methanesulfonate in Single Particles at an Inland Urban Location during a Phytoplankton Bloom, Environ. Sci. Technol., 44, 1566-

1572, http://doi.org/10.1021/es902069d, 2010.

Ghorai, S., Wang, B., Tivanski, A., and Laskin, A.: Hygroscopic properties of internally mixed particles composed of NaCl and water-soluble organic acids, Environ. Sci. Technol., 48, 2234-2241, http://doi.org/10.1021/es404727u, 2014.

Gross, D. S., Galli., M. E., Silva., P. J., and Prather., a. K. A.: Relative Sensitivity Factors for Alkali Metal and Ammonium Cations in Single-Particle Aerosol Time-of-Flight Mass Spectra, Anal. Chem., 72, 416-422, http://doi.org/10.1021/ac990434g, 2000.

Guasco, T. L., Cuadra-Rodriguez, L. A., Pedler, B. E., Ault, A. P., Collins, D. B., Zhao, D. F., Kim, M. J., Ruppel, M. J., Wilson, S. C., Pomeroy, R. S., Grassian, V. H., Azam, F., Bertram, T. H., and Prather, K. A.: Transition Metal Associations with Primary Biological Particles in Sea Spray Aerosol Generated in a Wave Channel, Environ. Sci. Technol., 48, 1324-1333, http://doi.org/10.1021/es403203d, 2014.

Healy, R. M., Sciare, J., Poulain, L., Kamili, K., Merkel, M., Müller, T., Wiedensohler, A., Eckhardt, S., Stohl, A., Sarda-Estève, R., McGillicuddy, E., amp, apos, Connor, I. P., Sodeau, J. R., and Wenger, J. C.: Sources and mixing state of size-resolved elemental carbon particles in a European megacity: Paris, Atmos. Chem. Phys., 12, 1681-1700, http://doi.org/10.5194/acp-12-1681-2012, 2012.

Hinz, K.-P., Trimborn, A., Weingartner, E., Henning, S., Baltensperger, U., and Spengler, B.: Aerosol single particle composition at the Jungfraujoch, J. Aerosol. Sci, 36, 123-145, http://doi.org/10.1016/j.jaerosci.2004.08.001, 2005.

Hughes, L. S., Allen, J. O., Bhave, P., Kleeman, M. J., Cass, G. R., Liu, D. Y., Fergenson, D. F., Morrical, B. D., and Prather, K. A.: Evolution of atmospheric particles along trajectories crossing the Los Angeles basin, Environ. Sci. Technol., 34, 3058-3068, http://doi.org/10.1021/es9908671, 2000.

Jayarathne, T., Sultana, C. M., Lee, C., Malfatti, F., Cox, J. L., Pendergraft, M. A., Moore, K. A., Azam, F., Tivanski, A. V., Cappa, C. D., Bertram, T. H., Grassian, V. H., Prather, K. A., and Stone, E. A.: Enrichment of saccharides and divalent cations in sea spray aerosol during two phytoplankton blooms, Environ. Sci. Technol., 50, 11511-11520, http://doi.org/10.1021/acs.est.6b02988, 2016.

Jeong, C. H., McGuire, M. L., Godri, K. J., Slowik, J. G., Rehbein, P. J. G., and Evans, G. J.: Quantification of aerosol chemical composition using continuous single particle measurements, Atmos. Chem. Phys., 11, 7027-7044, http://doi.org/10.5194/acp-11-7027-2011, 2011.

Kawamura, K., and Bikkina, S.: A review of dicarboxylic acids and related compounds in atmospheric aerosols: Molecular distributions, sources and transformation, Atmos. Res., 170, 140-160, http://doi.org/10.1016/j.atmosres.2015.11.018, 2016.

Knopf, D. A., Alpert, P. A., Wang, B., O'Brien, R. E., Kelly, S. T., Laskin, A., Gilles, M. K., and Moffet, R. C.: Microspectroscopic imaging and characterization of individually identified ice nucleating particles from a case field study, J. Geophys. Res. Atmos., 119, 10,365-310,381, http://doi.org/10.1002/2014jd021866, 2014.

Laskin, A., Moffet, R. C., Gilles, M. K., Fast, J. D., Zaveri, R. A., Wang, B., Nigge, P., and Shutthanandan, J.: Tropospheric chemistry of internally mixed sea salt and organic particles: Surprising reactivity of NaCl with weak organic acids, J. Geophys. Res. Atmos., 117, n/a-n/a, http://doi.org/10.1029/2012jd017743, 2012.

Li, L., Huang, Z., Dong, J., Li, M., Gao, W., Nian, H., Fu, Z., Zhang, G., Bi, X., Cheng, P., and Zhou, Z.: Real time bipolar time-of-flight mass spectrometer for analyzing single aerosol particles, Int. J. Mass Spectrom., 303, 118-124, http://doi.org/10.1016/j.ijms.2011.01.017, 2011.

Lightowlers, P. J., and Cape, J. N.: Sources and fate of atmospheric HCl in the U.K. and western Europe, Atmos. Environ., 22, 7-15, http://doi.org/10.1016/0004-6981(88)90294-6, 1988.

Lin, Q., Yang, Y., Fu, Y., Zhang, G., Jiang, F., Peng, L., Lian, X., Liu, F., Bi, X., Li, L., Chen, D., Li, M., Ou, J., Tang, M., Wang, X., Peng, P., amp, apos, an, and Sheng, G.: Enrichment of submicron sea-salt-containing particles in small cloud droplets based on single-particle mass spectrometry, Atmos. Chem. Phys., 19, 10469-10479, http://doi.org/10.5194/acp-19-10469-2019, 2019.

Ma, Q., Ma, J., Liu, C., Lai, C., and He, H.: Laboratory study on the hygroscopic behavior of external and internal C2-C4 dicarboxylic acid-NaCl mixtures, Environ. Sci. Technol., 47, 10381-10388, http://doi.org/10.1021/es4023267, 2013.

Ma, X., von Salzen, K., and Li, J.: Modelling sea salt aerosol and its direct and indirect effects on climate, Atmos. Chem. Phys., 8, 1311-1327, http://doi.org/doi.org/10.5194/acp-8-1311-2008, 2008.

Martin, A. C., Cornwell, G. C., Atwood, S. A., Moore, K. A., Rothfuss, N. E., Taylor, H., DeMott, P. J., Kreidenweis, S. M., Petters, M. D., and Prather, K. A.: Transport of pollution to a remote coastal site during gap flow from California's interior: impacts on aerosol composition, clouds, and radiative balance, Atmos. Chem. Phys., 17, 1491-1509, http://doi.org/10.5194/acp-17-1491-2017, 2017.

May, N. W., Gunsch, M. J., Olson, N. E., Bondy, A. L., Kirpes, R. M., Bertman, S. B., China, S., Laskin, A., Hopke, P. K., Ault, A. P., and Pratt, K. A.: Unexpected Contributions of Sea Spray and Lake Spray Aerosol to Inland Particulate Matter, Environ. Sci. Technol., 5, 405-412, http://doi.org/10.1021/acs.estlett.8b00254, 2018.

Mochida, M., Umemoto, N., Kawamura, K., and Uematsu, M.: Bimodal size distribution of C2-C4 dicarboxylic acids in the marine aerosols, J. Geophys. Res. Lett., 30, http://doi.org/10.1029/2003gl017451, 2003.

Nguyen, Q. T., Kjær, K. H., Kling, K. I., Boesen, T., and Bilde, M.: Impact of fatty acid coating on the CCN activity of sea salt particles, Tellus. B., 69, http://doi.org/10.1080/16000889.2017.1304064, 2017.

O'Dowd, C., Ceburnis, D., Ovadnevaite, J., Vaishya, A., Rinaldi, M., and Facchini, M. C.: Do anthropogenic, continental or coastal aerosol sources impact on a marine aerosol signature at Mace Head?, Atmos. Chem. Phys., 14, 10687-10704, http://doi.org/10.5194/acp-14-10687-2014, 2014.

Patterson, J. P., Collins, D. B., Michaud, J. M., Axson, J. L., Sultana, C. M., Moser, T., Dommer, A. C., Conner, J., Grassian, V. H., Stokes, M. D., Deane, G. B., Evans, J. E., Burkart, M. D., Prather, K. A., and Gianneschi, N. C.: Sea Spray Aerosol Structure and Composition Using Cryogenic Transmission Electron Microscopy, ACS. Cent. Sci. , 2, 40-47, http://doi.org/10.1021/acscentsci.5b00344, 2016.

Peng, C., Jing, B., Guo, Y. C., Zhang, Y. H., and Ge, M. F.: Hygroscopic Behavior of Multicomponent Aerosols Involving NaCl and Dicarboxylic Acids, J. Phys. Chem. A, 120, 1029-1038, http://doi.org/10.1021/acs.jpca.5b09373, 2016.

Prather, K. A., Bertram, T. H., Grassian, V. H., Deane, G. B., Stokes, M. D., DeMott, P. J., Aluwihare, L. I., Palenik, B. P., Azam, F., Seinfeld, J. H., Moffet, R. C., Molina, M. J., Cappa, C. D., Geiger, F. M., Roberts, G. C., Russell, L. M., Ault, A. P., Baltrusaitis, J., Collins, D. B., Corrigan, C. E., Cuadra-Rodriguez, L. A., Ebben, C. J., Forestieri, S. D., Guasco, T. L., Hersey, S. P., Kim, M. J., Lambert, W. F., Modini, R. L., Mui, W., Pedler, B. E., Ruppel, M. J., Ryder, O. S., Schoepp, N. G., Sullivan, R. C., and Zhao, D. F.: Bringing the ocean into the laboratory to probe the chemical complexity of sea spray aerosol, P. Natl. Acad. Sci. USA., 110, 7550-7555, http://doi.org/10.1073/pnas.1300262110, 2013.

Pratt, K. A., and Prather, K. A.: Mass spectrometry of atmospheric aerosolsuRecent developments and applications. Part II: On-line mass spectrometry techniques, Mass. Spectrom. Rev., 31, 17-48, http://doi.org/10.1002/mas.20330, 2012.

Qin, X., Bhave., P. V., and Prather., K. A.: Comparison of Two Methods for Obtaining

Quantitative Mass Concentrations from Aerosol Time-of-Flight Mass Spectrometry Measurements, Anal. Chem. , 78, 6169-6178, http://doi.org/10.1021/ac060395q, 2006.

Quinn, P. K., Collins, D. B., Grassian, V. H., Prather, K. A., and Bates, T. S.: Chemistry and related properties of freshly emitted sea spray aerosol, Chem. Rev., 115, 4383-4399, http://doi.org/10.1021/cr500713g, 2015.

Ryder, O. S., Ault, A. P., Cahill, J. F., Guasco, T. L., Riedel, T. P., Cuadra-Rodriguez, L. A., Gaston, C. J., Fitzgerald, E., Lee, C., Prather, K. A., and Bertram, T. H.: On the Role of Particle Inorganic Mixing State in the Reactive Uptake of N2O5 to Ambient Aerosol Particles, Environ. Sci. Technol., 48, 1618-1627, http://doi.org/10.1021/es4042622, 2014.

Ryder, O. S., Campbell, N. R., Morris, H., Forestieri, S., Ruppel, M. J., Cappa, C., Tivanski, A., Prather, K., and Bertram, T. H.: Role of organic coatings in regulating n2o5 reactive uptake to sea spray aerosol, J. Phys. Chem. A, 119, 11683-11692, http://doi.org/10.1021/acs.jpca.5b08892, 2015.

Song, X., and Hopke, P. K.: Classification of single particles analyzed by ATOFMS using an artificial neural network, ART-2A, Anal. Chem., 71, 860-865, http://doi.org/10.1021/ac9809682, 1999.

Srivastava, A., Pitesky., M. E., Steele., P. T., Tobias., H. J., Fergenson., D. P., Horn., J. M., Russell., S. C., Czerwieniec., G. A., Lebrilla., C. B., Gard., E. E., and Frank., M.: Comprehensive Assignment of Mass Spectral Signatures from Individual Bacillus atrophaeus Spores in Matrix-Free Laser

Desorption/Ionization Bioaerosol Mass Spectrometry, Anal. Chem. , 77, 3315-3323, http://doi.org/10.1021/ac048298p, 2005.

Sultana, C. M., Al-Mashat, H., and Prather, K. A.: Expanding Single Particle Mass Spectrometer Analyses for the Identification of Microbe Signatures in Sea Spray Aerosol, Anal. Chem., 89, 10162-10170, http://doi.org/10.1021/acs.analchem.7b00933, 2017a.

Sultana, C. M., Collins, D. B., and Prather, K. A.: Effect of Structural Heterogeneity in Chemical Composition on Online Single-Particle Mass Spectrometry Analysis of Sea Spray Aerosol Particles, Environ. Sci. Technol., 51, 3660-3668, http://doi.org/10.1021/acs.est.6b06399, 2017b.

Trueblood, J. V., Estillore, A. D., Lee, C., Dowling, J. A., Prather, K. A., and Grassian, V. H.: Heterogeneous Chemistry of Lipopolysaccharides with Gas-Phase Nitric Acid: Reactive Sites and Reaction Pathways, J. Phys. Chem. A., 120, 6444-6450, http://doi.org/10.1021/acs.jpca.6b07023, 2016.

Wang, B., and Laskin, A.: Reactions between water-soluble organic acids and nitrates in atmospheric aerosols: Recycling of nitric acid and formation of organic salts, J. Geophys. Res. Atmos., 119, 3335-3351, http://doi.org/10.1002/2013JD021169, 2014.

Wang, B., O'Brien, R. E., Kelly, S. T., Shilling, J. E., Moffet, R. C., Gilles, M. K., and Laskin, A.: Reactivity of liquid and semisolid secondary organic carbon with chloride and nitrate in atmospheric aerosols, J. Phys. Chem. A., 119, 4498-4508, http://doi.org/10.1021/jp510336q, 2015.

Wang, N., Lyu, X. P., Deng, X. J., Guo, H., Deng, T., Li, Y., Yin, C. Q., Li, F., and Wang, S. Q.: Assessment of regional air quality resulting from emission control in the Pearl River Delta region, southern China, Sci. Total. Environ., 573, 1554-1565, http://doi.org/10.1016/j.scitotenv.2016.09.013, 2016.

Wang, X. F., Deane, G. B., Moore, K. A., Ryder, O. S., Stokes, M. D., Beall, C. M., Collins, D. B., Santander, M. V., Burrows, S. M., Sultana, C. M., and Prather, K. A.: The role of jet and film drops in controlling the mixing state of submicron sea spray aerosol particles, P. Natl. Acad. Sci. USA., 114, 6978-6983, http://doi.org/10.1073/pnas.1702420114, 2017.

Wu, Z., Zhang, Y., Zhang, L., Huang, M., Zhong, L., Chen, D., and Wang, X.: Trends of outdoor air pollution and the impact on premature mortality in the Pearl River Delta region of southern China during 2006-2015, Sci. Total. Environ., 690, 248-260, http://doi.org/10.1016/j.scitotenv.2019.06.401, 2019.

Xiao, H.-s., Dong., J.-l., Wang., L.-y., Zhao., L.-j., Wang., F., and Zhang., Y.-h.: Spatially Resolved Micro-Raman Observation on the Phase Separation of Effloresced Sea Salt Droplets, Environ. Sci. Technol., 42, 8698–8702, http://doi.org/10.1021/es801181f, 2008.

Xu, G., Gao, Y., Lin, Q., Li, W., and Chen, L.: Characteristics of water-soluble inorganic and organic ions in aerosols over the Southern Ocean and coastal East Antarctica during austral summer, J. Geophys. Res. Atmos., 118, 13,303-313,318, http://doi.org/10.1002/2013jd019496, 2013.

Zawadowicz, M. A., Froyd, K. D., Murphy, D. M., and Cziczo, D. J.: Improved identification of primary biological aerosol particles using single-particle mass spectrometry, Atmos. Chem. Phys., 17, 7193-7212, http://doi.org/10.5194/acp-17-7193-2017, 2017.

Zhang, G., Lin, Q., Peng, L., Yang, Y., Fu, Y., Bi, X., Li, M., Chen, D., Chen, J., Cai, Z., Wang, X., Peng, P., Sheng, G., and Zhou, Z.: Insight into the in-cloud formation of oxalate based on in situ measurement by single particle mass spectrometry, Atmos. Chem. Phys., 17, 13891–13901, https://doi.org/10.5194/acp-17-13891-2017, 2017.

Zhao, Y., and Gao, Y.: Acidic species and chloride depletion in coarse aerosol particles in the US east coast, Sci. Total. Environ., 407, 541-547, http://doi.org/10.1016/j.scitotenv.2008.09.002, 2008.

Zhou, Y., Huang, X. H. H., Griffith, S. M., Li, M., Li, L., Zhou, Z., Wu, C., Meng, J., Chan, C. K., Louie, P. K. K., and Yu, J. Z.: A field measurement based scaling approach for quantification of major ions, organic carbon, and elemental carbon using a single particle aerosol mass spectrometer, Atmos. Environ., 143, 300-312, http://doi.org/10.1016/j.atmosenv.2016.08.054, 2016.

Figures

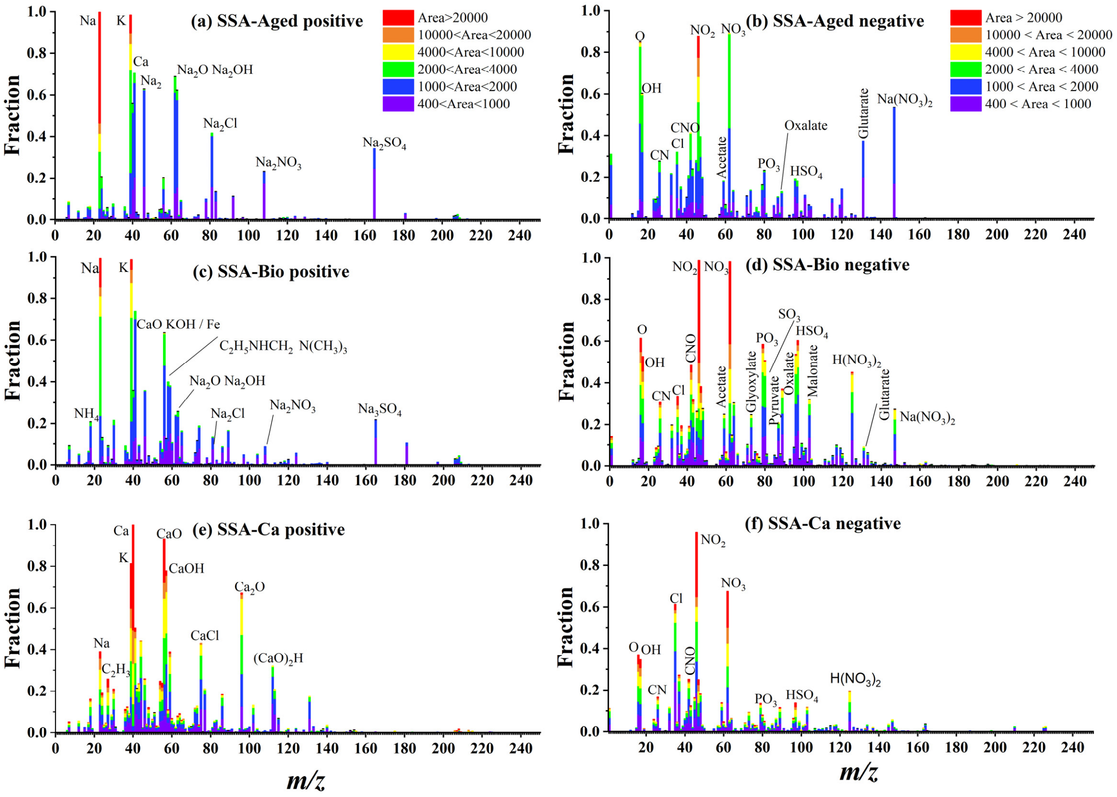

Figure 1. The averaged digitized positive and negative ion mass spectra of the major types of SSA particles.

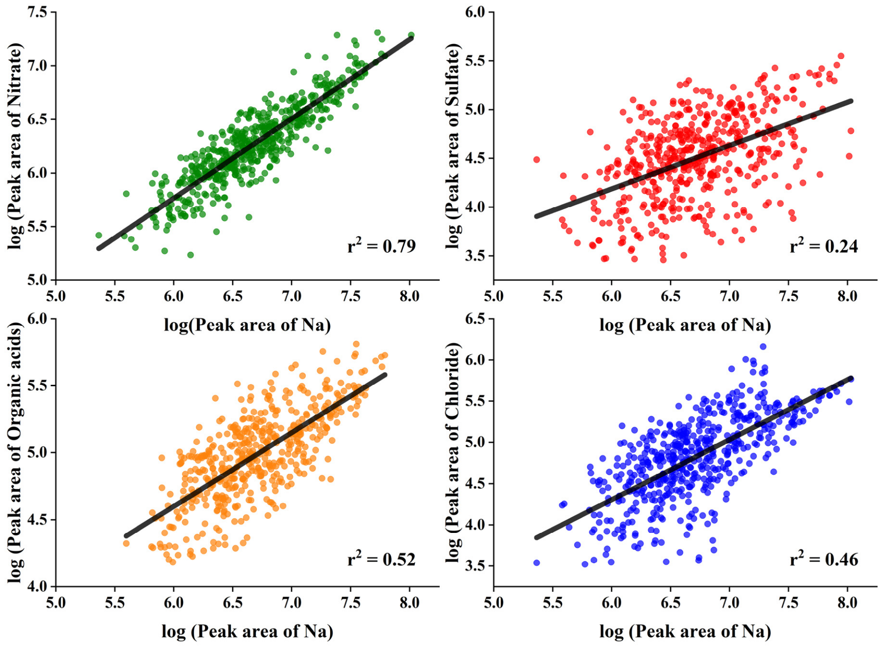

(a) SSA-Aged

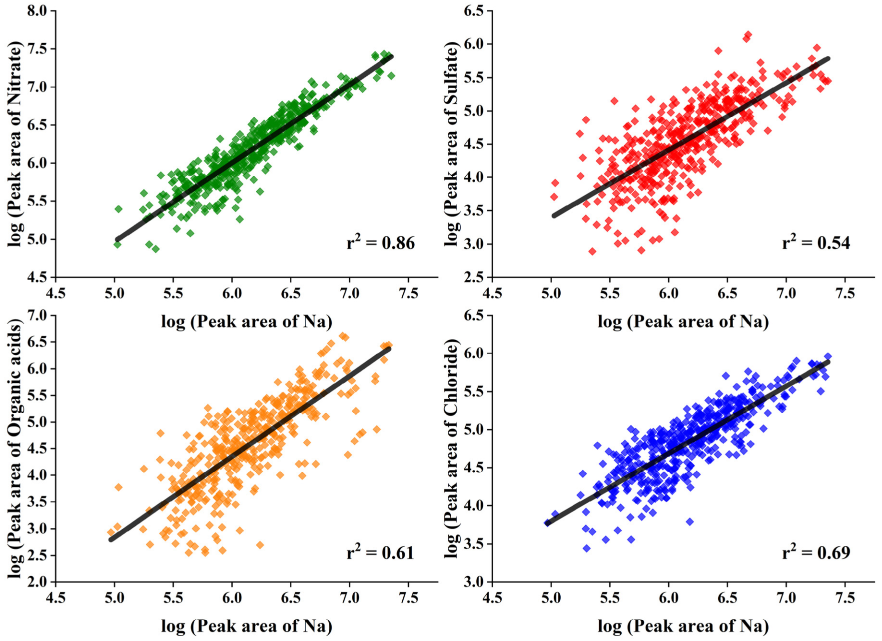

(b) SSA-Bio

Figure 2. Correlations between hourly mean peak area of Na (*m/z* 23) and sulfate (*m/z* -97), nitrate (*m/z* -46 and 62), organic acids (*m/z* -45, -59, -73, -87, -89, -103, -117 and -131) and chloride (*m/z* -35 and -37) in the SSA-Aged and SSA-Bio. The data is logarithmically transformed to follow a normal distribution.

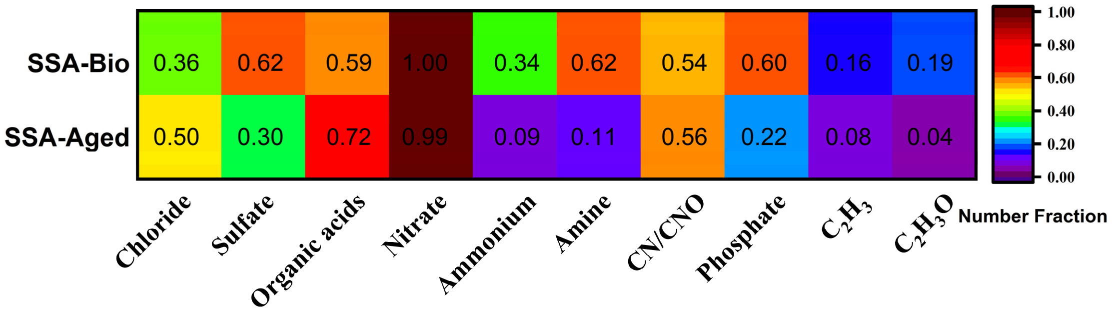

	Chloride	Sulfate	Organic acids	Nitrate	Ammonium	Amine	CN/CNO	Phosphate	C_2H_3	C_2H_3O
SSA-Bio	0.36	0.62	0.59	1.00	0.34	0.62	0.54	0.60	0.16	0.19
SSA-Aged	0.50	0.30	0.72	0.99	0.09	0.11	0.56	0.22	0.08	0.04

Figure 3. Hourly mean number fractions (NFs) of major component in the SSA-Aged and SSA-Bio. The major component includes chloride (*m/z* -35 or -37), sulfate (*m/z* -97), organic acids (*m/z* -45, -59, -73, -87, -89, -103, -117 or -131), nitrate (*m/z* -46 or -62), ammonium (*m/z* 18), amine (*m/z* 58 and 59), organic nitrogen (*m/z* -26 or -42), phosphate (*m/z* -63 or -79), and organic carbon (*m/z* 27 and 43).

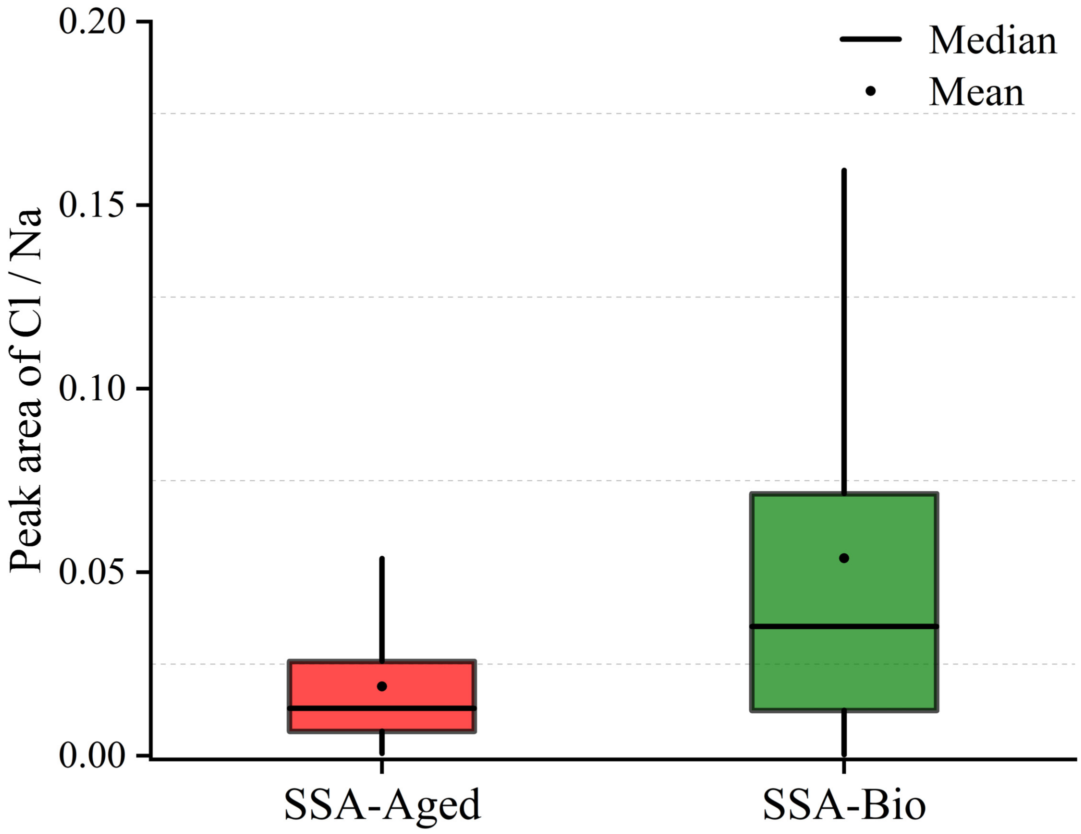

Figure 4. A box and whisker plot of hourly mean peak area of Cl / Na in SSA-Aged and SSA-Bio. Herein, the Cl / Na value is applied to evaluate the ageing degree of SSA particles. There is a significant difference of Cl / Na between the SSA-Aged and SSA-Bio (1.9% versus 5.4%, by mean value, respectively). In the box and whisker plot, the lower and upper lines of the box denote the 25 and 75 percentiles, respectively. The lower and upper edges denote the 10 and 90 percentiles, respectively.

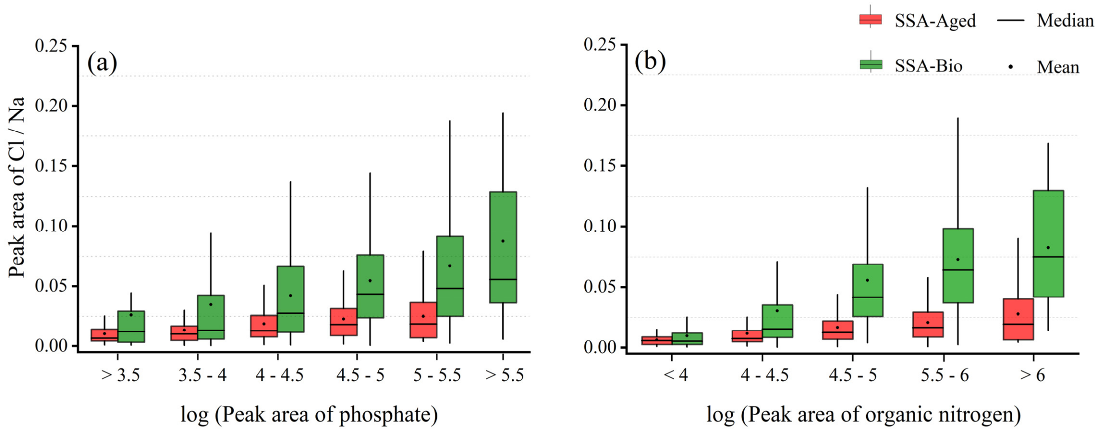

Figure 5. The hourly mean peak area ratio of Cl / Na varied as a function of logarithmical peak area of phosphate (*m/z* -63 and -79) and organic nitrogen (*m/z* -26 and -42).

Supplement of

Impact of organic acids on chloride depletion of inland transported sea spray aerosols

Bojiang Su et al.

**Correspondence to* : Lei Li (lileishdx@163.com)

1. Semi-quantitative analysis of SSA particles

Using single particle mass spectrometry (SPMS) alone is subjected to the transmission efficiencies of particles through the aerodynamic lens, the possible selectivity and matrix effects on chemical components, resulting in inaccuracies of the number concentration, size distribution and chemical composition of the ambient aerosols (Gross et al., 2000; Qin et al., 2006; Pratt and Prather, 2012).

Despite this, some species (e.g. sulfate, nitrate, sodium, ammonium, elemental carbon and organic carbon) presented relative strong correlations between peak area / relative peak area (data set from SPMS) and mass concentration (data set from other measurements such as micro-orifice uniform deposit impactor (MOUDI)), which indicated the real ambient condition could be reflected by SMPS in some extent (Qin et al., 2006; Jeong et al., 2011; Healy et al., 2012; Healy et al, 2013; Zhou et al., 2016). Besides, similar results of correlation analysis on Na^+, Cl^-, K^+ for SSA particles (< 2 µm) were also obtained, which suggested no significant additional composition effect for the desorption and ionization process (Dall'Osto et al., 2006).

In addition, for the core-shell structure of the most SSA particles (Collins et al., 2014; Chi et al., 2015), the pulse energy of the desorption and ionization laser via SPMS was influential for the selectivity of the detected components on the surface of the particles (Woods et al., 2002; Cai et al., 2006; Zelenyuk et al., 2008). Sultana et al. (2017) suggested that higher laser energy (> 1 mJ) could result in greater sodium signal, indicating more complete particle desorption and ionization. And lower laser energy (< 1 mJ) could be more likely to generate greater contribution to ion signature from the coating components such as organic species (Sultana et al., 2017). In order to reduce the impact of laser power on organic species, relative low laser energy (0.5 ± 0.05 mJ) was applied in this study.

Thus, a comparison analysis based on the obtained particle counts, size distributions and peak area / relative peak area via SPMAS in this study should be considered as the semi-quantitative analysis from statistical perspective (Hinz et al., 2005; Healy et al., 2012; Zhou et al., 2016).

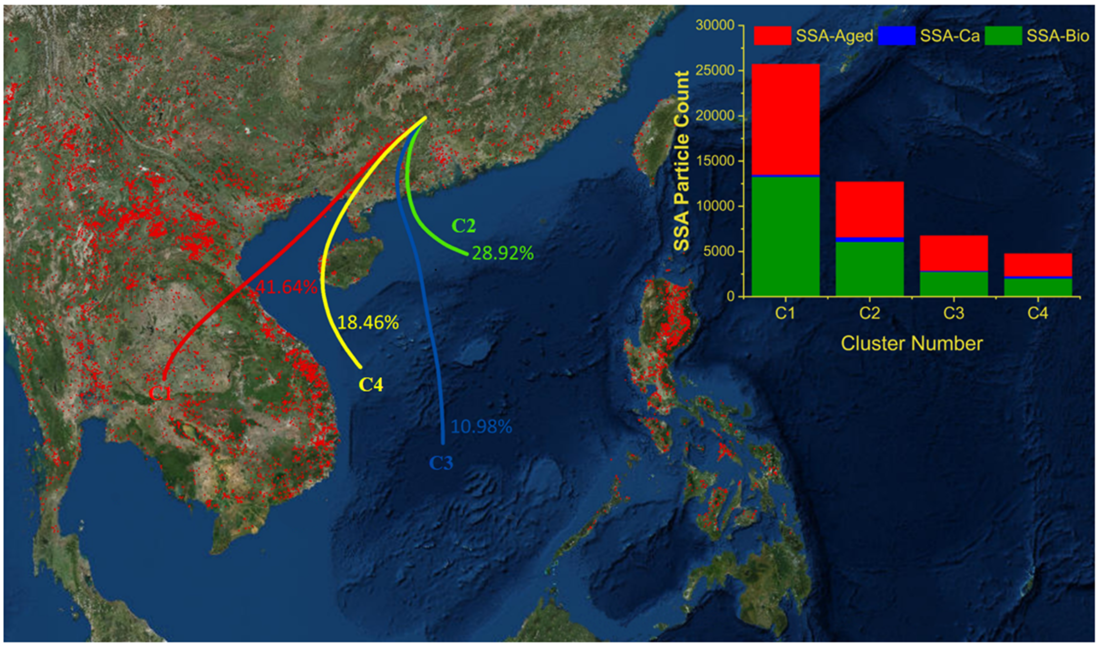

Figure S1. Quantitative distributions of SSA particles associated with clustered 72h back trajectories of air masses at 1800m above the ground during the sampling period (from 11 May to 3 June 2018). Four major cluster trajectories of air mass (namely C1, C2, C3, C4) were calculated by Meteoinfo (Wang, 2014) and plotted by Arcgis (Esri, Environmental Systems Research Institute, Inc.). Cluster 1 (41.64%) from Indo China Peninsula and Cluster 4 (18.46%) from south China Sea crossing through Hainan Peninsula carried the most (~ 25,000) and the least (~ 5,000) SSA particles, respectively. The both from the South China Sea Cluster 2 (28.92%) and Cluster 3 (10.98%), which brought approximately 12,500 and 7,500 SSA particles respectively, were rarely affected by anthropogenic emissions before reaching the coastline. Changes in proportions of the three types of SSA particles in different clusters were slight.

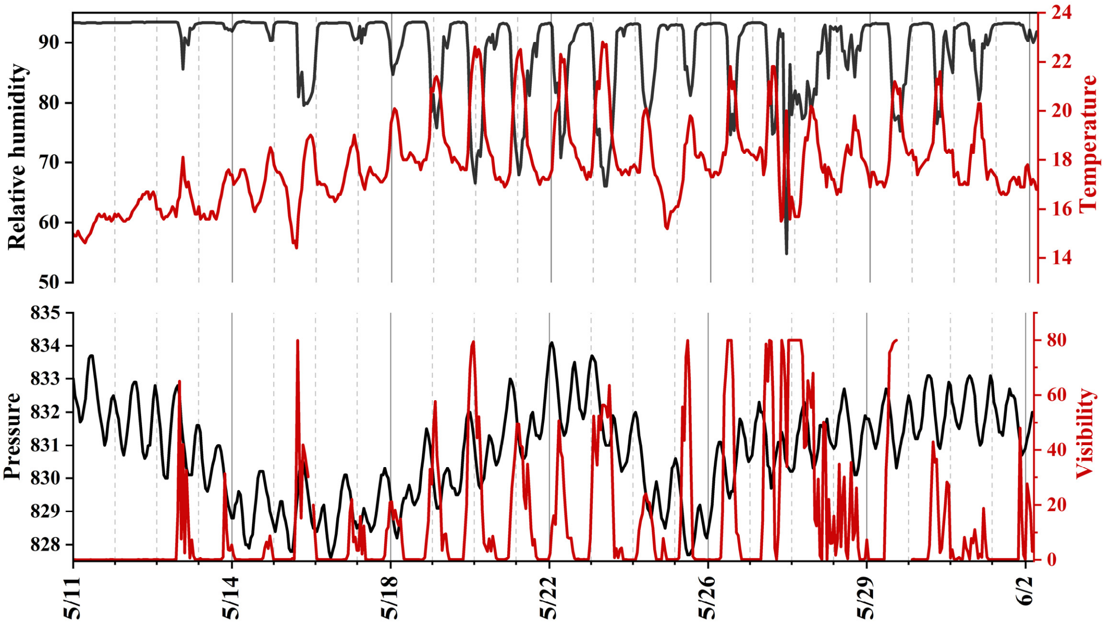

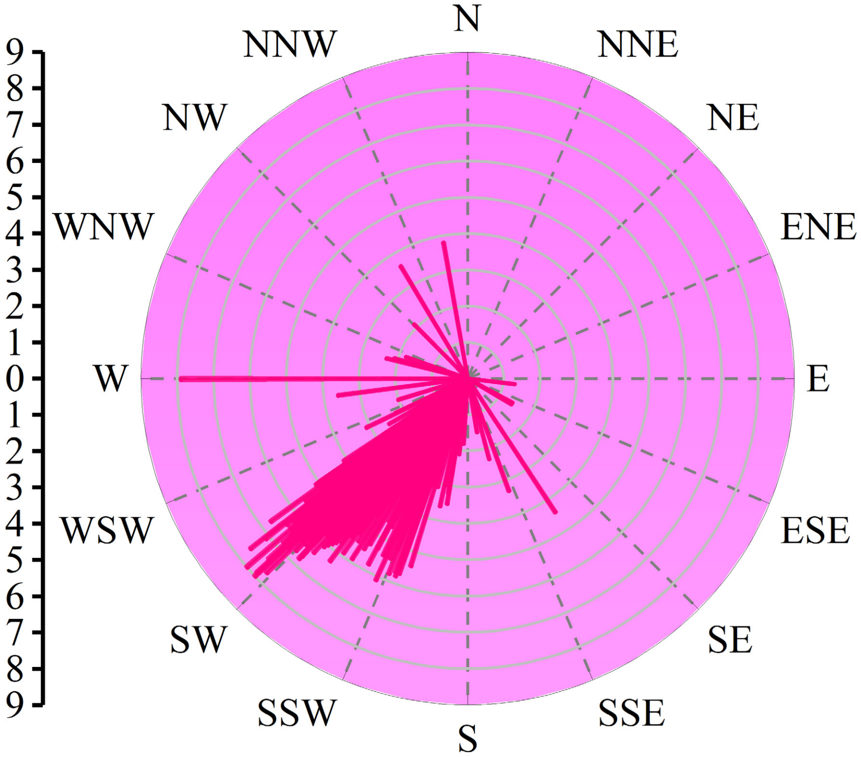

Fig S2. The hourly average variations in meteorological conditions and Wind Rose.

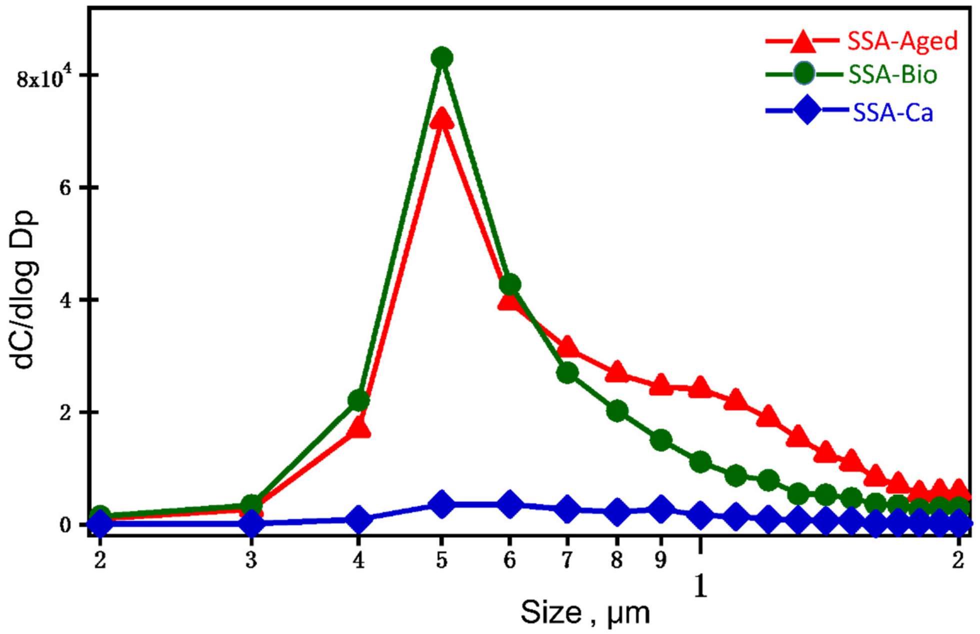

Figure S3. Unscaled size-resolved number distributions of major types of SSA particles during sampling period. SSA-Aged and SSA-Bio have similar trend in size range 0.2-2 µm, with approximately 70% of the particles concentrated in size range of 0.4-0.7 µm and peaked at size of 0.5 µm, suggesting that the both particle types may undergo the similar atmospheric chemical process. Such results indicate that SSA particles were aged during the inland transport and exhibited in fine particles. It is noted the results were only based on the size (d_{va}) range from 0.2 µm to 2 µm. There is a possibility that similar results were obtained for small particles ($d_{va} < 0.2$ µm).

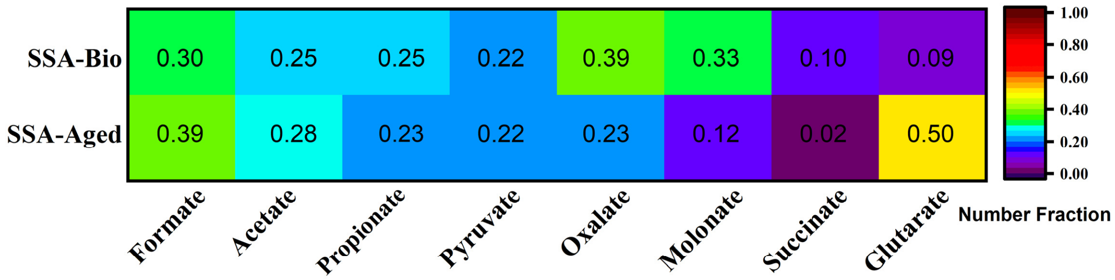

	Formate	Acetate	Propionate	Pyruvate	Oxalate	Molonate	Succinate	Glutarate
SSA-Bio	0.30	0.25	0.25	0.22	0.39	0.33	0.10	0.09
SSA-Aged	0.39	0.28	0.23	0.22	0.23	0.12	0.02	0.50

Figure S4. Hourly mean number fractions (NFs) of all detected organic acids in SSA-Aged and SSA-Bio, which included formate (*m/z* -45), acetate (*m/z* -59), propionate (*m/z* -73), pyruvate (*m/z* -87), oxalate (*m/z* -89), molonate (*m/z* -103), succinate (*m/z* -117) and glutarate (*m/z* -131).

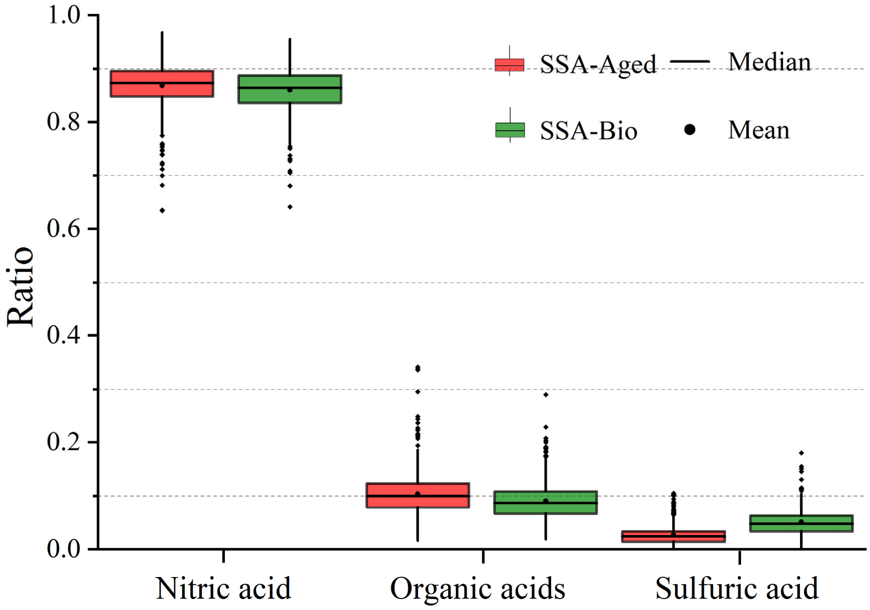

Figure S5. The relative contribution of different acids (nitric acid, sulfuric acid, and organic acids) to the chloride depletion of SSA particles. The ratio referred to the hourly mean relative peak area (RPA) ratio (acids / (sulfate + nitrate + organic acids)). Sulfate, nitrate and organic acids referred to peaks at m/z -97, m/z -46 and -62, and the mentioned organic acids in Fig. S4, respectively.

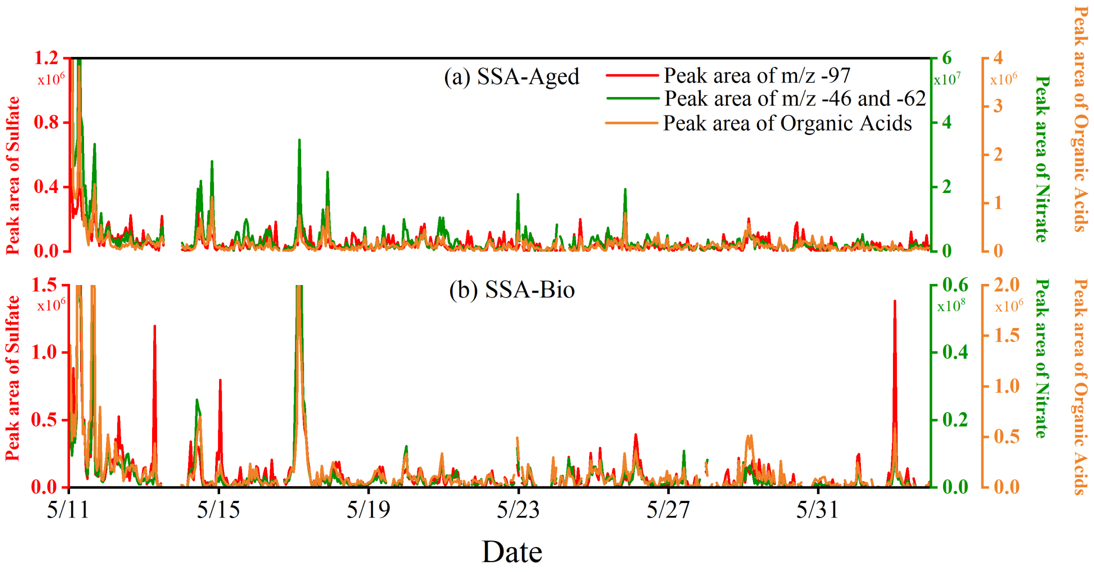

Figure S6. Hourly variations in the peak areas of sulfate (*m/z* -97), nitrate (*m/z* -46 and -62) and organic acids (sum of the mentioned organic acids in Fig. S4) in SSA-Aged and SSA-Bio during whole sampling period.

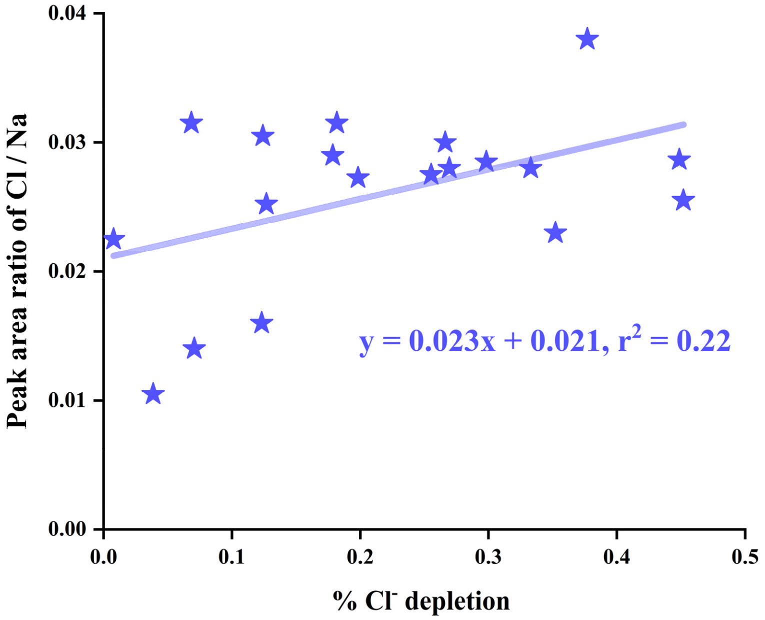

Fig S7. Correlation analysis of the both assessment methods of chloride depletion. These data were conducted significance test and $p < 0.001$. The correlation analysis was carried out on 19 among 22 set of data due to the rest of the maximum, minimum and the abnormal value (detailed in Table S1).

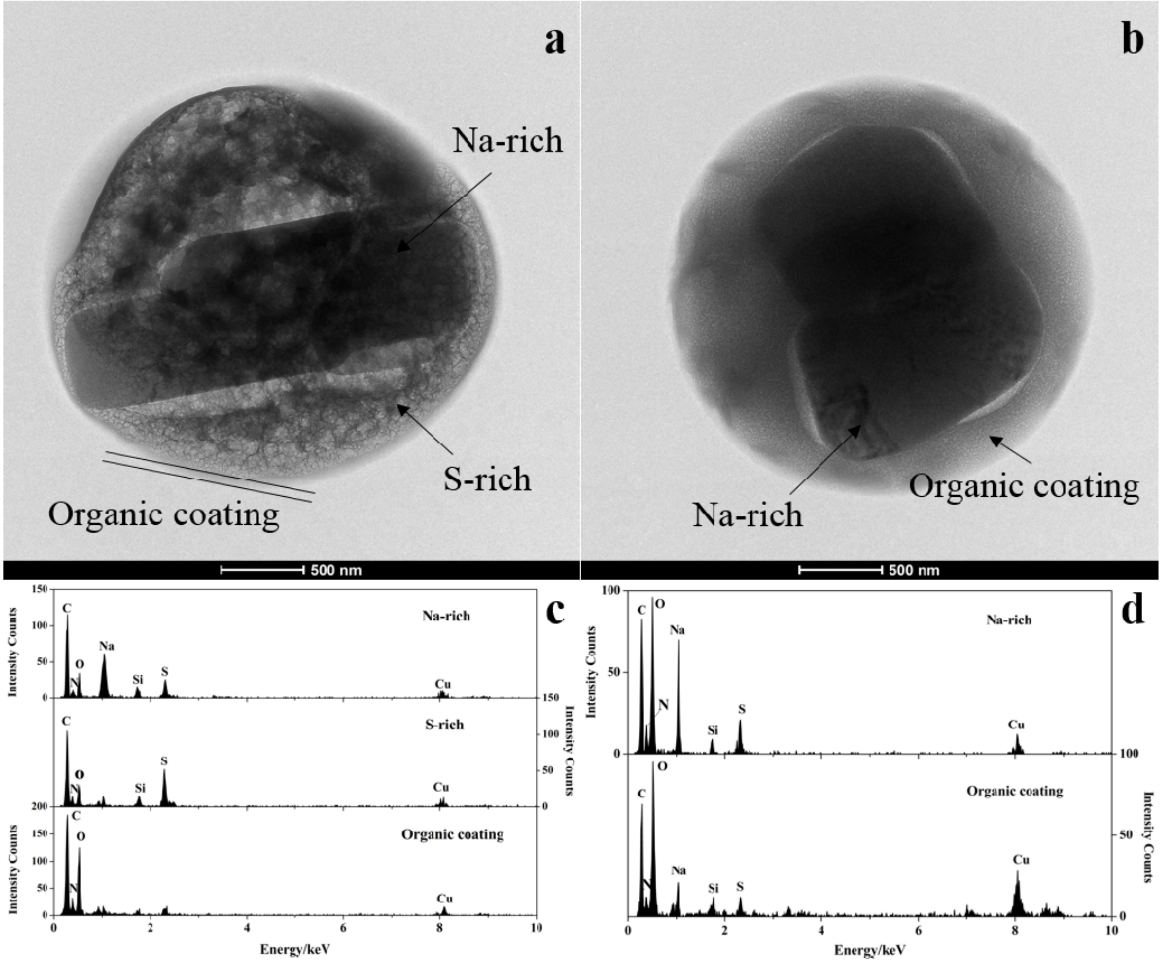

Figure S8. Transmission electron microscopy (TEM) images and energy dispersive X-ray (EDX) spectra of individual particles with coating of various thickness. These particles contained abundant Na and kept the crystalline phase with its irregular shape, which were regarded as SSA particles (Chi et al., 2015). High energy electron beams by TEM / EDS could cause the loss of volatile components, such as nitrate. This typical transparent coating with high C and O indicated a possible organic coating, and Na-rich core completely surrounded by the organic coating.

Sampling set names	**Sampling dates**	**Duration (min)**	**Na^+**	**Ca^{2+}**	**Cl^-**	**NO_3^-**	**SO_4^{2-}**	**Cl^-% depletion**	**Peak area ratio of Cl / Na**
Cloud Water 1	May 11	480	0.24	0.01	0.16	1.26	1.81	0.64	0.005*
Cloud Water 2	May 26	150	1.31	0.74	0.58	5.59	9.32	0.65	0.023
Cloud Water 3	May 26	140	1.73	0.98	0.56	3.90	6.48	0.74	0.028
Cloud Water 4	May 26	180	5.24	1.80	0.99	6.41	9.65	0.87	0.025
Cloud Water 5	May 27	214	1.98	1.21	1.08	9.33	13.84	0.55	0.029
Cloud Water 6	May 30	270	1.85	1.35	0.53	8.57	13.08	0.73	0.030
Cloud Water 7	May 30	305	1.88	1.07	0.79	11.14	16.95	0.67	0.028
Cloud Water 8	May 30	515	1.68	1.22	0.83	11.59	19.32	0.55	0.026
Cloud Water 9	Jun 1	225	1.07	0.79	0.31	5.57	5.71	0.73	0.028
Cloud Water 10	Jun 2	230	0.99	0.42	0.05	2.10	3.84	0.96	0.011
Cloud Water 11	Jun 2	141	1.63	0.59	0.30	3.84	5.64	0.88	0.016
Cloud Water 12	Jun 2	134	1.44	0.46	0.15	1.85	2.63	0.93	0.014
Cloud Water 13	Jun 2	203	3.79	1.03	0.35	3.85	5.80	0.94	0.046*
$PM_{2.5}$ 1	May 14-15	1440	1.12	1.04	0.38	1.05	2.60	0.62	0.038
$PM_{2.5}$ 2	May 18-19	1406	1.46	0.47	0.40	1.80	4.75	0.82	0.032
$PM_{2.5}$ 3	May 19-20	1423	0.45	0.22	0.07	2.07	5.09	0.88	0.031
$PM_{2.5}$ 4	May 20-21	1366	0.70	0.22	0.21	3.22	4.70	0.80	0.027
$PM_{2.5}$ 5	May 21-22	1431	0.48	0.18	0.13	2.11	3.52	0.82	0.029
$PM_{2.5}$ 6	May 22-23	1414	0.57	0.16	0.06	0.97	2.94	0.93	0.032
$PM_{2.5}$ 7	May 24-25	1419	0.72	0.21	0.17	2.59	4.22	0.80	0.054*
$PM_{2.5}$ 8	May 26-27	1391	0.72	0.47	0.25	2.36	3.20	0.70	0.029
$PM_{2.5}$ 9	May 29-30	1421	0.51	0.03	0.01	0.35	1.84	0.99	0.023
Mean			1.43	0.67	0.38	4.16	6.68	0.78	0.026

* These data are excluded because of the maximum (0.054), minimum (0.005) and abnomal value (0.046).

Table S1. The major ions, chloride depletion (%Cl$^-$) and hourly mean peak area ratio of Cl / Na in the sample of cloud water and PM$_{2.5}$ during sampling period. The mass concentrations (μg m^{-3}) of Na$^+$, Ca^{2+}, Cl$^-$, NO$_3^-$ and SO$_4^{2-}$ were analyzed using an ion chromatography (Metrohm, Herisau, Switzerland). The cloud water was sampled by a Caltech Active Strand Cloud Water Collector Version 2 (CASCC2) (Modini et al., 2015), when visibility was < 3 km until the volume exceeded 250 ml. The PM2.5 was sampled using an Atmospheric particle sampler (Mingye Environmental Protection Technology Co., Ltd., China) with an inlet cyclone with a cut-off aerodynamic diameter of 2.5 μm.

References

Cai, Y., Zelenyuk., A., and Imre., D.: A High Resolution Study of the Effect of Morphology On the Mass Spectra of Single PSL Particles with Na-containing Layers and Nodules, Aerosol. Sci. Tech, 40, 1111–1122, http://doi.org/10.1080/02786820601001677, 2006.

Chi, J. W., Li, W. J., Zhang, D. Z., Zhang, J. C., Lin, Y. T., Shen, X. J., Sun, J. Y., Chen, J. M., Zhang, X. Y., Zhang, Y. M., and Wang, W. X.: Sea salt aerosols as a reactive surface for inorganic and organic acidic gases in the Arctic troposphere, Atmos. Chem. Phys., 15, 11341-11353, http://doi.org/10.5194/acp-15-11341-2015, 2015.

Collins, D. B., Zhao, D. F., Ruppel, M. J., Laskina, O., Grandquist, J. R., Modini, R. L., Stokes, M. D., Russell, L. M., Bertram, T. H., Grassian, V. H., Deane, G. B., and Prather, K. A.: Direct aerosol chemical composition measurements to evaluate the physicochemical differences between controlled sea spray aerosol generation schemes, Atmos. Meas. Tech., 7, 3667-3683, http://doi.org/10.5194/amt-7-3667-2014, 2014.

Gross, D. S., Galli., M. E., Silva., P. J., and Prather., a. K. A.: Relative Sensitivity Factors for Alkali Metal and Ammonium Cations in Single-Particle Aerosol Time-of-Flight Mass Spectra, Anal. Chem., 72, 416-422, http://doi.org/10.1021/ac990434g, 2000.

Healy, R. M., Sciare, J., Poulain, L., Kamili, K., Merkel, M., Müller, T., Wiedensohler, A., Eckhardt, S., Stohl, A., Sarda-Estève, R., McGillicuddy, E., amp, apos, Connor, I. P., Sodeau, J. R., and Wenger, J. C.: Sources and mixing state of size-resolved elemental carbon particles in a European megacity: Paris, Atmos. Chem. Phys., 12, 1681-1700, http://doi.org/10.5194/acp-12-1681-2012, 2012.

Healy, R. M., Sciare, J., Poulain, L., Crippa, M., Wiedensohler, A., Prévôt, A. S. H., Baltensperger, U., Sarda-Estève, R., McGuire, M. L., Jeong, C. H., McGillicuddy, E., amp, apos, Connor, I. P., Sodeau, J. R., Evans, G. J., and Wenger, J. C.: Quantitative determination of carbonaceous particle mixing state in Paris using single-particle mass spectrometer and aerosol mass spectrometer measurements, Atmos. Chem. Phys., 13, 9479-9496, http://doi.org/10.5194/acp-13-9479-2013, 2013.

Hinz, K.-P., Trimborn, A., Weingartner, E., Henning, S., Baltensperger, U., and Spengler, B.: Aerosol single particle composition at the Jungfraujoch, J. Aerosol. Sci, 36, 123-145, http://doi.org/10.1016/j.jaerosci.2004.08.001, 2005.

Jeong, C. H., McGuire, M. L., Godri, K. J., Slowik, J. G., Rehbein, P. J. G., and Evans, G. J.: Quantification of aerosol chemical composition using continuous single particle measurements, Atmos. Chem. Phys., 11, 7027-7044, http://doi.org/10.5194/acp-11-7027-2011, 2011.

Modini, R. L., Frossard, A. A., Ahlm, L., Russell, L. M., Corrigan, C. E., Roberts, G. C., Hawkins, L. N., Schroder, J. C., Bertram, A. K., Zhao, R., Lee, A. K. Y., Abbatt, J. P. D., Lin, J., Nenes, A., Wang, Z., Wonaschütz, A., Sorooshian, A., Noone, K. J., Jonsson, H., Seinfeld, J. H., Toom-Sauntry, D., Macdonald, A. M.,and Leaitch, W. R.: Primary marine aerosol-cloud interactions off the coast of California, J. Geophys. Res., 120, 4282–4303, http://doi.org/10.1002/2014JD022963, 2015.

Pratt, K. A., and Prather, K. A.: Mass spectrometry of atmospheric aerosolsuRecent developments and applications. Part II: On-line mass spectrometry techniques, Mass. Spectrom. Rev., 31, 17-48, http://doi.org/10.1002/mas.20330, 2012.

Qin., X., Bhave., P. V., and Prather., K. A.: Comparison of Two Methods for Obtaining Quantitative Mass Concentrations from Aerosol Time-of-Flight Mass Spectrometry Measurements, Anal. Chem. , 78, 6169-6178, http://doi.org/10.1021/ac060395q, 2006.

Reents, W. D., and Ge, Z.: Simultaneous Elemental Composition and Size Distributions of Submicron Particles in Real Time Using Laser Atomization Ionization Mass Spectrometry, Aerosol. Sci. Tech., 33, 122-134, http://doi.org/10.1080/027868200410886, 2000.

Reents, W. D., and Schabel., M. J.: Measurement of Individual Particle Atomic Composition by Aerosol Mass Spectrometry, Anal. Chem. , 73, 5403-5414, http://doi.org/10.1021/ac010436c, 2001.

Song, X., and Hopke, P. K.: Classification of single particles analyzed by ATOFMS using an artificial neural network, ART-2A, Anal. Chem., 71, 860-865, http://doi.org/10.1021/ac9809682, 1999.

Sultana, C. M., Collins, D. B., and Prather, K. A.: Effect of Structural Heterogeneity in Chemical Composition on Online Single-Particle Mass Spectrometry Analysis of Sea Spray Aerosol Particles, Environ Sci Technol, 51, 3660-3668, http://doi.org/10.1021/acs.est.6b06399, 2017.

Wang, Y. Q.: MeteoInfo: GIS software for meteorological data visualization and analysis, Meteorol. Appl., 21, 360–368, https://doi.org/10.1002/met.1345, 2014.

Zelenyuk, A., Yang., J., Song., C., Zaveri., R. A., and Imre., D.: “Depth-Profiling” and Quantitative Characterization of the Size, Composition, Shape, Density, and Morphology of Fine Particles with SPLAT, a Single-Particle Mass Spectrometer, J. Phys. Chem. A 112, 669-677, http://doi.org/10.1021/jp077308y, 2008.

Zhou, Y., Huang, X. H. H., Griffith, S. M., Li, M., Li, L., Zhou, Z., Wu, C., Meng, J., Chan, C. K., Louie, P. K. K., and Yu, J. Z.: A field measurement based scaling approach for quantification of major ions, organic carbon, and elemental carbon using a single particle aerosol mass spectrometer, Atmos. Environ., 143, 300-312, http://doi.org/10.1016/j.atmosenv.2016.08.054, 2016.